

Particle size, shape and distribution

4.1 PARTICLE SIZE

The size of a spherical homogeneous particle is uniquely defined by its diameter. For a cube the length along one edge is characteristic, and for other regular shapes there are equally appropriate dimensions. With some regular particles, it may be necessary to specify more than one dimension. For example: cone, diameter and height; cuboid, length, width and height.

Derived diameters are determined by measuring a size-dependent property of the particle and relating it to a linear dimension. The most widely used of these are the equivalent spherical diameters. Thus, a unit cube has the same volume as a sphere of diameter 1.24 units, hence this is the derived volume diameter.

If an irregularly shaped particle is allowed to settle in a liquid, its terminal velocity may be compared with the terminal velocity of a sphere of the same density settling under similar conditions. The size of the particle is then equated to the diameter of the sphere. In the laminar flow region, the particle moves with random orientation, but outside this region it orients itself to give maximum resistance to motion so that the free-falling diameter for an irregular particle is greater in the intermediate region than in the laminar flow region. The free-falling diameter, in the laminar flow region, becomes the Stokes diameter. Stokes' equation can be used for spherical particles, up to a Reynolds number of 0.2, at which value it will give a diameter under-estimation of about 2%. Above 0.2 corrections have to be applied. Corrections may also be applied for non-spherical particles, so that the derived diameter is independent of settling conditions becoming purely a function of particle size. These diameters are particularly useful for characterizing suspended particles in the atmosphere and other cases where the settling behaviour of suspended solids is being examined.

For irregular particles, the assigned size usually depends upon the method of measurement, hence the particle sizing technique should, wherever possible, duplicate the process one wishes to control. Thus, for paint pigments, the projected area is important, while for chemical reactants, the total surface area should be determined. The projected area diameter may be determined by microscopy for each individual particle, but surface area is usually deter-

mined for a known weight or volume of powder. The magnitude of this surface area will depend on the method of measurement, permeametry, for example, giving a much lower area than gas adsorption. The latter gives the surface area accessible to the gas molecules and, therefore, depends on the size of the gas molecules if the solid contains very small pores.

The sieve diameter, for square-mesh sieves, is the length of the side of the minimum square aperture through which the particle will pass, though this definition needs modification for sieves which do not have square apertures. In a sieving operation, such a particle will not necessarily pass through the appropriate mesh, particularly if it will only pass through when presented in a particular orientation as with elongated particles. For all such particles to pass through, the sieving time would approach infinity. There is also a range of aperture sizes in any sieve mesh and certain particles may only pass through the largest apertures.

Microscopy is the only widely used particle-sizing technique in which individual particles are observed and measured. A single particle has an infinite number of linear dimensions, and it is only when they are averaged that a meaningful value results; this is similar for a large number of particles. When a linear dimension is measured parallel to some fixed direction (Martin, Feret, unrolled or shear diameter), the size distribution of these measurements reflects the size distribution of the projected areas of the particles. These are called statistical diameters. Comparing the projected area of the particle with series of circles, gives a diameter which describes that particle for the orientation in which it is measured. In microscopy, this is usually the projected area diameter in stable orientation but, in certain cases, the particle may rest in an unstable position to give a lower value. Some definitions of particle size are given in Table 4.1.

These diameters are usually applied to an assembly of particles and distri-

Table 4.1 Definitions of particle size

Symbol	Name	Definition	Formula
d_v	Volume diameter	Diameter of a sphere having the same volume as the particle	$V = \frac{\pi}{6} d_v^3$
d_s	Surface diameter	Diameter of a sphere having the same surface as the particle	$S = \pi d_s^2$
d_{sv}	Surface volume diameter	Diameter of a sphere having the same external surface to volume ratio as a sphere	$d_{sv} = \frac{d_v^3}{d_s^2}$
d_d	Drag diameter	Diameter of a sphere having the same resistance to	$F_D = C_D A \rho_f \frac{v^2}{2}$

Table 4.1 (Cont.)

Symbol	Name	Definition	Formula
d_f	Free-falling diameter	motion as the particle in a fluid of the same viscosity and at the same velocity (d_d approximates to d_s when Re is small)	where $C_D A = f(d_d)$ $F_D = 3\pi d_d \eta v$ $Re < 0.2$
d_{St}	Stokes' diameter	Diameter of a sphere having the same density and the same free-falling speed as the particle in a fluid of the same density and viscosity	$d_{St}^2 = \frac{d_v^3}{d_d}$
d_a	Projected area diameter	The free-falling diameter of a particle in the laminar flow region ($Re < 0.2$)	$A = \frac{\pi}{4} d_a^2$
d_p	Projected area diameter	Diameter of a circle having the same area as the projected area of the particle resting in a stable position	Mean value for all possible orientations $d_p = d_s$ for convex particles
d_c	Perimeter diameter	Diameter of a circle having the same area as the projected area of the particle in random orientation	
d_A	Sieve diameter	Diameter of a circle having the same perimeter as the projected outline of the particle	
d_F	Feret's diameter	The width of the minimum square aperture through which the particle will pass	
d_M	Martin's diameter	The mean value of the distance between pairs of parallel tangents to the projected outline of the particle	
d_R	Unrolled diameter	The mean chord length through the centre of gravity of the particle	$E(d_R) = \frac{1}{\pi} \int_0^{2\pi} d_R d\theta_R$

butions are quoted in terms of the measured or derived diameters. Particles having the same diameter can have vastly different shapes, therefore one parameter should not be considered in isolation.

A single particle can have an infinite number of statistical diameters, hence these diameters are only meaningful when sufficient particles have been measured to give average statistical diameters in each size range.

For a single particle, the expectation of a statistical diameter and its coefficient of variation may be calculated from the following equations [1] (see figure 4.1):

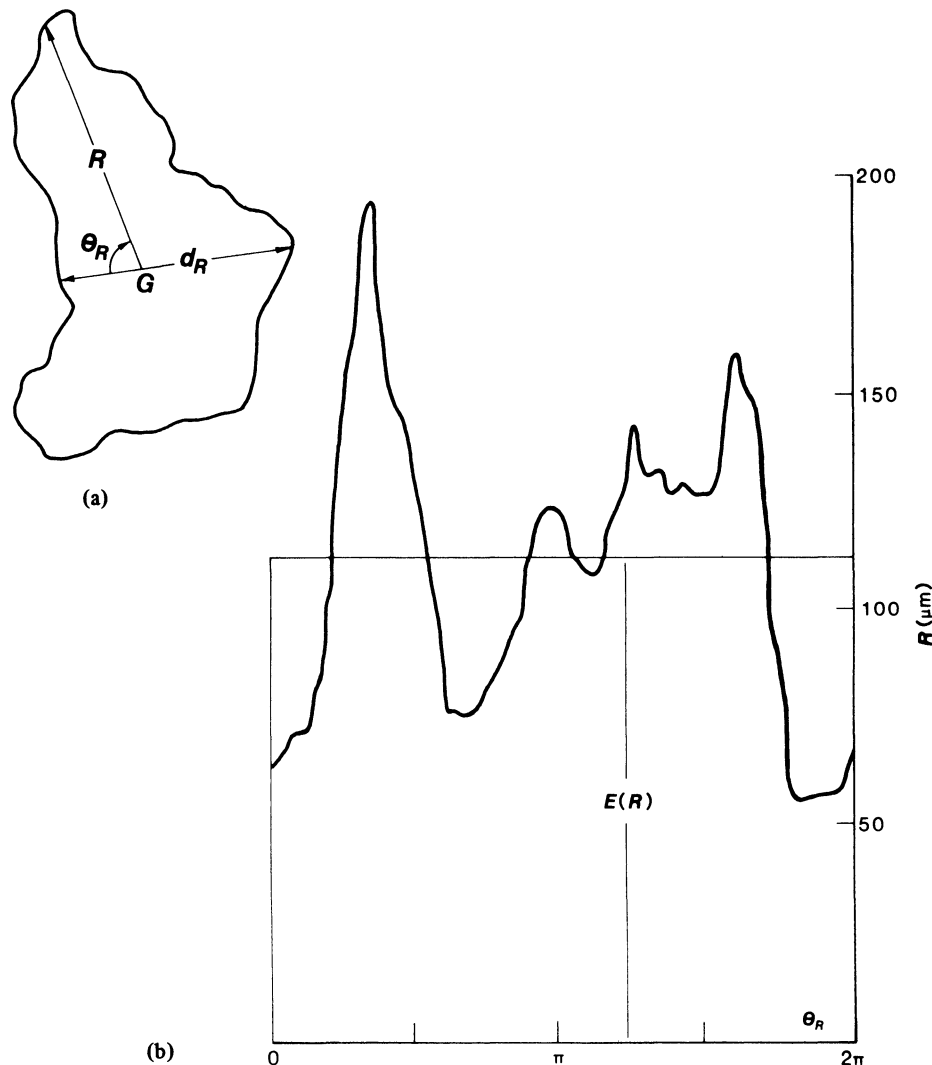


Figure 4.1 (a) Definition of unrolled diameter d_R and radius R ; (b) unrolled curve [1].

$$E(d_R) = \frac{1}{\pi} \int_0^{2\pi} R d\theta_R \quad (4.1)$$

$$\sigma_R = \sqrt{\left[E(R^2) - \frac{E^2(R)}{E(R)} \right]} \quad (4.2)$$

$$E(d_F) = \frac{1}{\pi} \int_0^\pi d_F d\theta_F \quad (4.3)$$

$$\sigma_F = \sqrt{\left[E(d_F^2) - \frac{E^2(d_F)}{E(d_F)} \right]} \quad (4.3a)$$

$$E(d_M) = \frac{1}{\pi} \int_0^\pi d_M d\theta_M \quad (4.4)$$

$$\sigma_M = \sqrt{\left[E(d_M^2) - \frac{E^2(d_M)}{E(d_M)} \right]} \quad (4.4a)$$

4.2 PARTICLE SHAPE

It is known that particle shape influences such properties as the flowability of powders, packing, interaction with fluids and the covering power of pigments, although little quantitative work has been carried out on these relationships. Qualitative terms may be used to give some indication of the nature of particle shape and some of these, extracted from the British Standard 2955: Glossary of Terms Relating to Powders, are given in Table 4.2.

Table 4.2 Definitions of particle shape

Acicular	needle-shaped
Angular	sharp-edged or having roughly polyhedral shape
Crystalline	freely developed in a fluid medium of geometric shape
Dentritic	having a branched crystalline shape
Fibrous	regularly or irregularly thread-like
Flaky	plate-like
Granular	having approximately an equidimensional irregular shape
Irregular	lacking any symmetry
Modular	having rounded, irregular shape
Spherical	global shape

Such general terms are inadequate for the determination of shape factors that can be incorporated as parameters into equations concerning particle

properties where shape is involved as a factor. In order to do this, it is necessary to be able to measure and define shape quantitatively.

In recent years there has been an upsurge of interest in particle shape analysis using pattern recognition techniques [79–81] in which input data are categorized into classes. The potential use of these techniques [82] and the use of the decision function in morphological analysis have been introduced.

There are two points of view regarding the assessment of particle shape. One is that the actual shape is unimportant and all that is required is a number for comparison purposes. The other is that it should be possible to regenerate the original particle shape from the measurement data.

The numerical relations between the various ‘sizes’ of a particle depend on particle shape, and dimensionless combinations of the sizes are called shape factors. The relations between measured sizes and particle volume or surface are called shape coefficients.

4.2.1 Shape coefficients

There are two especially important properties of particles, surface and volume, and these are proportional to the square and cube respectively of some characteristic dimension. The constants of proportionality depend upon the dimension chosen to characterize the particle; the projected area diameter is used in the following discussion.

$$\text{Surface of particles, } S = \pi d_s^2 = \alpha_{s,a} d_a^2 = x_s^2 \quad (4.5)$$

$$\text{Volume of particle, } V = \frac{\pi}{6} d_v^3 = \alpha_{v,a} d_a^3 = x_v^3 \quad (4.6)$$

where α_s and α_v are the surface and volume shape coefficients, the additional suffix denoting that the measured diameter is the projected area diameter. The symbol x denotes size, as opposed to diameter, and includes the shape coefficient. This artifact is found to be very useful for general treatment of data.

The surface area per unit volume (the volume-specific surface) is the ratio S to V :

$$S_V = \frac{\alpha_{sv,a}}{d_a} = \frac{6}{d_{sv}} = \frac{1}{x_{sv}} \quad (4.7)$$

Further, the volume-specific surface by microscopy is defined as:

$$S_{V,a} = \frac{6}{d_a} \quad (4.8)$$

One line of approach to the use of shape coefficients was given by Heywood [2] who recognized that the word 'shape' in common usage refers to two distinct characteristics of a particle. These two characteristics should be defined separately, one by the degree to which the particle approaches a definite form such as a cube, tetrahedron or sphere, and the second by the relative proportions of the particle which distinguish one cuboid, tetrahedron or spheroid from another of the same class.

When three mutually perpendicular dimensions of a particle may be determined, Heywood's ratios [3] may be used:

$$\text{elongation ratio } n = L/B \quad (4.9)$$

$$\text{flakiness ratio } m = B/T \quad (4.10)$$

where

- (a) the thickness T is the minimum distance between two parallel planes which are tangential to opposite surfaces of the particle, one plane being the plane of maximum stability.
- (b) the breadth B is the minimum distance between two parallel planes which are perpendicular to the planes defining the thickness and are tangential to opposite sides of the particle.

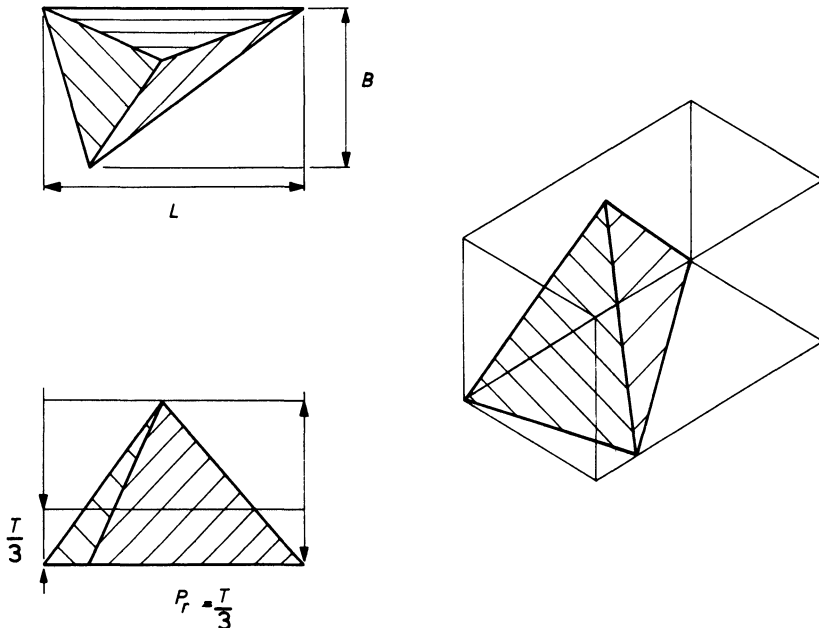


Figure 4.2 Heywood's dimensions.

- (c) the length L is the distance between two parallel planes which are perpendicular to the planes defining thickness and breadth and are tangential to opposite sides of the particle.

Consider a particle circumscribed by a rectangular parallelepiped of dimensions L by B by T , then:

$$\text{projected area of the particle } A = \frac{\pi}{4} d_a^2 = \alpha_a B L \quad (4.11)$$

where α_a is the area ratio.

Volume of particle equals projected area by mean thickness:

$$\alpha_{v,a} d_a^3 = \alpha_a B L p_r T \quad (4.12)$$

where p_r is the prismoidal ratio (see figure 4.2).

Combining equations (4.11) and (4.12) gives:

$$\alpha_{v,a} = \frac{\pi \sqrt{\pi}}{8} \frac{p_r}{m \sqrt{\alpha_a} n} \quad (4.13)$$

If the particle is equidimensional, i.e. $B = L = T$ and $n = m = 1$, then the volume coefficient takes on a special value α_e where:

$$\alpha_e = \frac{\pi \sqrt{\pi}}{8} \frac{p_r}{\sqrt{\alpha_a}} \quad (4.14)$$

Thus, α_e may be used to define particle form. When the particle is not equidimensional, the appropriate value of $\alpha_{v,a}$ is $\alpha_e/m\sqrt{n}$ which substantiates the reasoning given earlier that shape is a combination of the proportions and geometrical form.

Heywood classified particles into tetrahedral, prismoidal, sub-angular and rounded. Values of α and p_r for these classes are given in Table 4.3 [4].

$\alpha_{v,a}$ can be calculated using equation (4.12) combined with direct obser-

Table 4.3 Values of α and p_r for particles of various shapes

Shape group	α_a	p_r
Angular {	0.5 – 0.8	0.4 – 0.53
prismoidal	0.5 – 0.9	0.53–0.9
Sub-angular	0.65–0.85	0.55–0.8
Rounded	0.72–0.82	0.62–0.75

Table 4.4 Values of α_{ea} and C for various geometrical forms and also for irregular particles

Shape group	α_{ea}	C
Geometrical forms		
tetrahedral	0.328	4.36
cubical	0.696	2.55
spherical	0.524	1.86
Approximate forms		
angular { tetrahedral	0.38	3.3
prismoidal	0.47	3.0
sub-angular	0.51	2.6
rounded	0.54	2.1

vation to determine the shape group into which the particle fits and the values of m and n . This is practicable down to sizes as small as 5 μm by measurements on the number, mean size, weight and density of closely graded fractions. Indeed, $\alpha_{v,a}$ may be determined directly by weighing a known number of particles of known mean size.

$\alpha_{s,a}$ is more difficult to determine, but Heywood developed the following relationship on the basis of a large number of experimental measurements:

$$\alpha_{s,a} = 1.57 + C \left(\frac{\alpha_{ea}}{m} \right)^{\frac{4}{3}} \frac{n+1}{n} \quad (4.15)$$

in which C is constant depending upon geometrical form. Table 4.4 shows the values of α_{ea} and C for various geometrical forms and also for irregular particles.

4.2.2 Shape factors

If it is required to define the size of a particle by a single dimension, it is usual to do so by expressing the size in terms of one of the diameters defined in Table 4.1. The variation between these diameters increases as the particles diverge more from the spherical shape, and hence shape is an important factor in the correlation of sizing analyses made by various procedures.

One of the earliest defined shape factors is the sphericity (ψ_w) which was defined by Wadell [5–8] as:

$$\psi_w = \frac{\text{surface area of a sphere having the same volume as the particle}}{\text{surface area of the particle}} \quad (4.16)$$

$$\psi_w = \left(\frac{d_v}{d_s} \right)^2$$

At low Reynolds number and with convex particles, the drag diameter equals the surface diameter and the Stokes diameter (d_{St}) is defined as:

$$\begin{aligned} d_{St} &= \left[\frac{d_v^3}{d_s} \right]^{\frac{1}{2}} \\ &= \psi_w^{1/4} d_v \end{aligned} \quad (4.17)$$

Further, the surface-volume mean diameter is given by:

$$\begin{aligned} d_{sv} &= \frac{d_v^3}{d_s^2} \\ &= \psi_w d_v \end{aligned} \quad (4.18)$$

For microscope analysis Laird [19] prefers the definition:

$$\psi_L = \frac{S_o}{S_p} \quad (4.19)$$

where S_o is the surface area of a sphere with a diameter equal to the equivalent diameter and S_p is the surface area of the particle computed from the measured surface area.

For rounded images, whose principal dimensions in two directions at right angles to each other are a and b , Heywood [2] quotes the semi-empirical formula for the equivalent diameter:

$$d_e = \left(\frac{4}{\pi} \times 0.77ab \right)^{\frac{1}{2}} \quad (4.20)$$

For rectangular images the following equation yields a result which is only 1% different from the one calculated above.

$$d_e = (ab)^{\frac{1}{2}} \quad (4.21)$$

Particles rest on microscope slides in the position of greatest stability. Cylindrical particles, of length kd where d is the cross-sectional diameter, would be expected to rest with the axis horizontal for $k > 1$ and vertical for $k < 1$. Laird found that this was so and that a region existed, $0.85 > k > 1.5$, where both orientations were adopted.

For discs or cylinders with $k < 0.85$:

$$\psi_L = \frac{2k}{1 + 2k} \quad (4.22)$$

For cylinders with $k > 1.5$:

Table 4.5 Relationship between shape coefficients and particle shape for cylindrical particles of unit diameter cross-section

k	d_v	d_s	d_{St}	$\psi_w^{-1} = \frac{\alpha_{sv,c}}{6} \frac{\alpha_{sv,St}}{6}$	ψ_L^{-1}
0.125	0.572	0.791	0.485	1.912	1.620
0.25	0.721	0.866	0.658	1.443	1.316
0.50	0.909	1.000	0.867	1.210	1.156
1	1.145	1.225	1.107	1.145	1.107
2	1.442	1.581	1.377	1.202	1.148
4	1.817	2.121	1.682	1.363	1.262
8	2.289	2.915	2.028	1.622	1.437

$$\Psi_L = \frac{2}{1 + 2k} \quad (4.23)$$

(see Table 4.5). Laird also determined sphericity from sieving and sedimentation studies.

Krumbein's [9, 10] definition of sphericity is:

$$\psi_K^3 = \left(\frac{C}{B}\right)\left(\frac{B}{L}\right)^2 \quad (4.24)$$

where L is the longest dimension of the particle, the breadth B is measured perpendicular to this, and C is the particle thickness. (Note: these definitions are different to Heywood's.)

Hausner [12] proposed a method of assessing particle shape by comparing the particle with an enveloping rectangle of minimum area. If the rectangle length is a and its width is b , three characteristics are defined:

$$\text{The elongation ratio } x = a/b \quad (4.25)$$

$$\text{The bulkiness factor } y = A/ab \quad (4.26)$$

$$\text{The surface factor } z = C^2/12.6A \quad (4.27)$$

where A is the projected area of the particle and C is its perimeter.

Medalia [13] represents the particle in three dimensions as an ellipsoid with radii of gyration equal to those of the particle and defines an anisometry in terms of the ratios of the radii.

Church [14] proposed the use of the ratio of the expected values (see equations 4.3 and 4.4) of Martin's and Feret's diameters as a shape factor for

a population of elliptical particles. Cole [15] introduced an image-analysing computer (the Quantimet 720) to compare longest chord, perimeter and area for large numbers of particles. Many other methods have been proposed and reviewed by Pahl *et al.* [16], and Davies [17], Beddow [18] and Laird [19].

4.2.3 Applications of shape factors and shape coefficients

If an analysis is carried out by two different techniques, the two results can be brought into coincidence by multiplying by a shape factor provided that particle shape does not change with particle size. For example, if the median size by Coulter analysis is 32 µm and by gravitational sedimentation is 29.2 µm, multiplying the sedimentation (Stokes) diameters by [32/29.2] will yield the Coulter distribution.

This ratio is in itself a shape factor, but it can be extended by writing the alternative form of Stokes' diameter (see Table 4.1):

$$\left(\frac{d_{St}}{d_c}\right)^2 = \frac{d_v^3}{d_s} \frac{I}{d_v^2} = \frac{d_v}{d_s} = \left(\frac{29.2}{32}\right)^2$$

Hence, from equation (4.16):

$$\psi_w = 0.693$$

If microscopic examination reveals the form of the particles to be cylindrical, for example, of length kd where d is the cross-sectional diameter, then the relationship between k , α_{sv} and ψ can be found since:

$$S = (\frac{1}{2} + k)\pi d^2 = \pi d_s^2$$

$$V = \frac{\pi}{4}kd^3 = \frac{\pi}{6}d_v^3$$

Hence, the Coulter diameter, $d_c = d_v = 3d\sqrt{(\frac{3}{2}k)}$

the surface diameter, $d_s = d\sqrt{k + 0.5}$

the Stokes diameter, $d_{St} = \sqrt{\frac{d_v^3}{d_s}} = \left(\frac{9k^2}{2(1 + 2k)}\right)^{\frac{1}{4}}d$

the sphericity, $\psi_w = \frac{(18k^2)^{\frac{1}{3}}}{(1 + 2k)}$

the surface-volume shape coefficient from sedimentation data,

$$\alpha_{sv,St} = \left(\frac{2 + 4k}{k}\right)\left(\frac{d_{St}}{d}\right) = \left[\frac{3}{k}\right]^{\frac{1}{2}}[2(1 + 2k)]^{\frac{3}{4}}$$

the surface-volume shape coefficient from Coulter data,

$$\begin{aligned} a_{sv,c} &= \left(\frac{2 + 4k}{k} \right) \left(\frac{d_v}{d} \right) \\ &= \left[\frac{3}{2k^2} \right]^{\frac{1}{3}} (2 + 4k) \end{aligned}$$

It can be shown that:

Table 4.6 Calculated values of shape coefficients

Form	Proportions	Linear dimension used as d_r	$a_{s,r}$	$a_{v,r}$	$a_{sv,r}$
Sphere		diameter	3.14	0.52	6.00
Spheroid	1:1:2	minor axis	5.37	1.05	5.13
	1:2:2	minor axis	8.67	2.09	4.14
	1:1:4	minor axis	10.13	2.09	4.83
	1:4:4	minor axis	28.50	8.38	3.40
Ellipsoid	1:2:4	shortest axis	15.86	4.19	3.79
	height = diameter	diameter	4.71	0.79	6.00
Cylinder	height = 2 diameters	diameter	7.85	1.57	5.00
	height = 4 diameters	diameter	14.14	3.14	4.50
	height = $\frac{1}{2}$ diameter	diameter	3.14	0.39	8.00
	height = $\frac{1}{4}$ diameter	diameter	2.36	0.20	12.00

Table 4.7 Measured values of surface-volume shape coefficient

Material	Approximate sizes	a_{sv}	Specific surface method	Particle size method
Alumina	15–45	16		
Coal	15–90	12–17	permeametry	microscope
Dolomite	25–45	11		(d_a)
Silica	15–70	11		
Tungsten carbide	15–45	14		
Coal	15–90	10–12	permeametry	Coulter counter (d_v)
Silica	15–70	9		
Coal	0.5–10	9–11	light weight	
Diamond	0.5–12	8	extinction	count (d_v)
Quartz	0.5–10	9		

Tables 4.6 and 4.7 are from BS 4359 (1970); Part 3, reproduced by permission of the British Standards Institution, 2 Park Street, London W.1, from whom copies of the complete standard may be obtained.

$$\frac{\alpha_{sv,c}}{6} = \frac{1}{\psi_w}$$

Data, for unit diameter cylinders, are presented in Table 4.5. Data for other shapes are presented in Tables 4.6 and 4.7. From these it can be seen that $\alpha_{sv}/6$ and ψ_w^{-1} are both at a minimum when the shape is most compact ($k = 1$) and increase as the particles become rod-shaped ($k > 1$) or flaky ($k < 1$).

For the numerical illustration, when $\psi^{-1} = 1.44$, $\alpha_{sv,c}/6 = 1.32$ and $k = 0.25$ or 5.5. A visual examination will reveal whether the particles are flaky or rod-shaped.

Example

Consider two cuboids of similar shape but different sizes, i.e. side lengths 1 : 2 : 3 and 2 : 4 : 6:

maximum projected areas	6 + 24;	$A = 30$
total surface areas	22 + 88;	$S = 110$
total volume	6 + 48;	$V = 54$
projected area diameter		$A = \frac{\pi}{4}n\bar{d}_a^2 ; \quad \bar{d}_a = 4.36$
mean surface diameter		$S = \pi n\bar{d}_s^2 ; \quad \bar{d}_s = 4.18$
surface shape coefficient		$S = \alpha_{s,a}n\bar{d}_a^2 ; \quad \alpha_{s,a} = 2.9$
mean volume diameter		$V = \frac{\pi}{6}n\bar{d}_v^3 ; \quad \bar{d}_v = 3.72$
volume shape coefficient		$V = \alpha_{v,a}n\bar{d}_a^3 ; \quad \alpha_{v,a} = 0.326$
surface-volume mean diameter		$d_{sv} = \frac{d_v^3}{d_s^2} ; \quad \bar{d}_{sv} = 2.94$
volume-specific surface		$S_v = \frac{S}{V} = \frac{6}{d_{sv}} ; \quad S_v = 2.04$
volume-specific surface by microscopy	$S_{v,a}$	$S_{v,a} = \frac{6}{\bar{d}_a} ; \quad S_{v,a} = 1.37$

(See BS 4359 (1970): Part 3, for further examples.)

The surface-volume shape coefficient has been determined for quartz and silica from surface area measurements using nitrogen adsorption giving $14 < \alpha_{sv} < 18$ with no significant variation with particle size. Fair and Hatch [21] found that by measuring smoothed surfaces, values of $\alpha_{sv,a}$ as low as 7

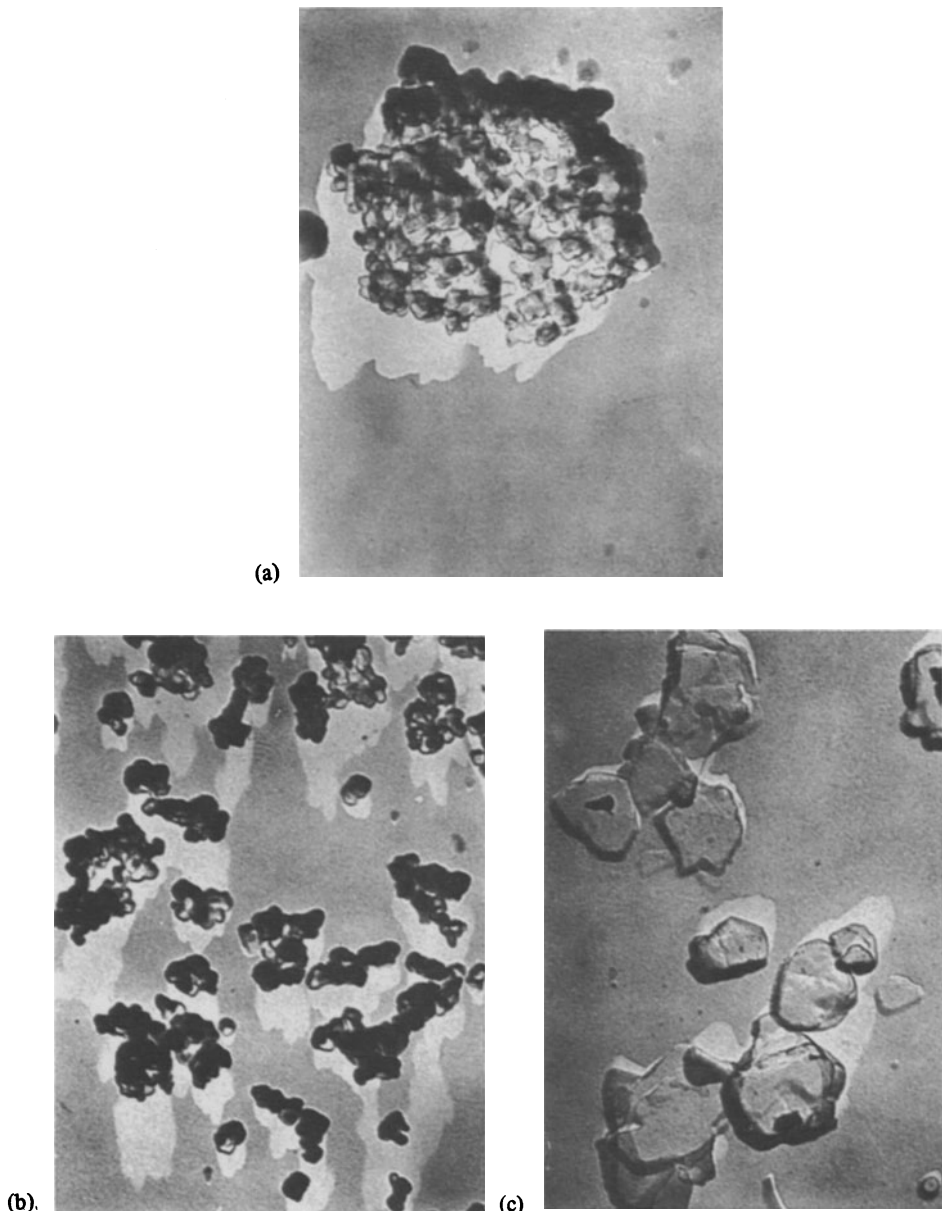


Figure 4.3 Electron photomicrographs of two paint pigments, showing how particles can be aggregates of finer particles (Crowl [22]). (a) A single particle of Prussian blue about $1\text{ }\mu\text{m}$ in diameter. The nitrogen adsorption surface area is $61.3\text{ m}^2\text{ g}^{-1}$ from which the surface-volume mean diameter is $0.051\text{ }\mu\text{m}$. This is seen to be the diameter of the individual primary particles of which the aggregate is made up. Similarly, the micronized Prussian blue (b) has approximately the same surface-volume mean diameter. (c) With the red oxide the diameter is $0.21\text{ }\mu\text{m}$ which is approximately the same as the solid particle seen in the micrograph.

were found ($\alpha_{sv,a} = 6$ for spheres). Crowl [22] found that with Prussian blue, the specific surface by nitrogen adsorption applied to the primary particles of which each single particle is made up (see figure 4.3). With red iron oxide, however, the specific surface applied to the single primary particle.

The mean volume shape may be determined from a knowledge of the number, mean size, weight and density of the particles composing a fraction graded between close limits. Further, if the surface area is determined by permeametry, a surface shape may be evaluated through this will differ from that obtained from the gas adsorption surface area. Hence, when any shape is quoted, the method of obtaining it should also be given.

Ellison [23] obtained the value 0.9 for the ratio of the sizes of silica particles determined by settling experiments and mounted in agar in random orientation. Hodkinson [24] found, from measurements of quartz particles by light scattering, a diameter ratio of 0.8 between particles in a liquid suspension and settled particles. Cartwright [57] attempted to find the magnitude of the differences in mean projected diameters between particles of quartz in random and stable orientation by microscopy. He used four different mounting techniques and found no significant differences. This, he attributed to the difficulty in mounting particles in random orientation. These factors for the mean ratio of projected diameter for random and stable orientation are indicative of the properties of the powder and are therefore of use to the analyst.

Respirable coal mine dust samples from three different US mines were classified into four fractions using a Bahco [68]. Shape factors were determined as ratios of the following diameters from microscopy:

$$\bar{d}_a = \left[\frac{\sum n d_a^2}{\sum n} \right]^{\frac{1}{2}}$$

A_p from photosedimentation with correction for extinction coefficient, N_w from microscopy:

$$\bar{d}_p = \left[\frac{4A_p}{\pi N_w} \right]^{\frac{1}{2}}$$

$$\left(A_p = \frac{\pi}{4} \sum n d_p^2 \right)$$

S_w from krypton gas adsorption, N_w from microscopy:

$$\bar{d}_{BET} = \left[\frac{S_w}{\pi N_w} \right]^{\frac{1}{2}}$$

ρ from density measurement, N_w from microscopy:

$$\bar{d}_{sv} = \frac{3}{2\rho A_p}$$

where N_w = number of particles/unit weight

A_p = projected area of particles, in random orientation, per unit weight. See Table 4.1 for definitions of other symbols.

It was postulated that a relationship might exist between shape and the incidence of pneumoconiosis.

A method, for shape determination, has been described in which the image analysis system consists of an Optronics scanning microdensitometer and a computer program [58]. It performs quantitative measurements of particle size distribution, shape and edge texture from photographs, where shape is defined as perimeter divided by projected area. A full analysis takes about three and a half man-hours and its most successful application has been in the analysis of silica sands in deep bed air filters for the removal of radioactive particulates. A relationship was found between collection efficiency and edge texture [59].

A device has been described to measure the degree of equi-axial deviation of powder particles as a ratio between longitudinal and transverse axes [69]. The determination is based on measuring the flow of rarified gas in two mutually perpendicular directions.

Kaye [70] describes a method using spatial filtering by which a particular particle of known shape and size can be detected among a background of other particles.

An examination of the shape distribution of sugar crystals has also been carried out using a modified Zeiss-Endter particle size analyser [71]. Shape was defined by Wadell's shape factor and by length to width ratio.

4.2.4 Shape indices

Tsubaki and Jimbo [1, 25, 26] argue that many of the proposed shape factors had little practical applicability to the analysis of real powders until the advent of electronic techniques and the computer. They define six shape indices based on ratios of the following diameters (see Table 4.1): d_a , d_c , d_F , d_R . The shape indices are: ψ_{ac} , ψ_{aF} , ψ_{aR} , ψ_{cF} , ψ_{cR} , ψ_{FR} , where, for example, $\psi_{ac} = d_a/d_c$. They defined the statistical diameters and coefficients of variation according to equations (4.1) to (4.4).

Furthermore, the elongation was used for study.

$$Z = d_{F_{\pi/2}}/d_{F_{\min}} \quad (4.28)$$

where $d_{F_{\min}}$ = the minimum value of the Feret diameter and $d_{F_{\pi/2}}$ = the diameter perpendicular to this.

They later added three more indices ψ_{Fa} , ψ_{Stkv} and κ . The arithmetic average of breadth and length is defined as follows:

$$d_{\bar{F}} = \frac{1}{2}(d_{F_{\min}} + d_{F_{n/2}}) \quad (4.29)$$

The dynamic shape factor κ is defined as the ratio of the resistance to motion of a given particle divided by the resistance of a spherical particle of the same volume. When the particle is settling under laminar flow conditions:

$$\kappa = \left(\frac{d_v}{d_{St}} \right)^2 \quad (4.30)$$

Since this is a squared term which for comparison purposes they wished to reduce to unit power they introduced the shape factor $\psi_{St} = d_{St}/d_v$. [Note $\kappa = \psi_w^{-1/2}$ where ψ_w is Wadell's sphericity factor.]

For non-re-entrant particles, according to Cauchy's theorem, $d_a = E(d_F)$ and ψ_{Fa} has a maximum value of 1.0 for circles, rectangles and other convex shapes; it is therefore very useful for indicating the extent of concavities.

Ψ_{Ra} , Ψ_{aF} , Ψ_{RF} , σ_R , σ_F and Z were found to mainly show the slimness of the particles, the best indicators being σ_F and Z in that order.

Ψ_{Hc} and ψ_{Rc} were found to correspond poorly with particle morphology.

4.2.5 Shape regeneration by Fourier analysis

Briefly, this method consists of finding the particle outline and its centre of gravity from which a polar co-ordinate system is set up. Standard Fourier transform techniques are then used to generate the Fourier coefficients A_n and their associated angles θ_n .

In 1969 Schwarcz and Shane [27] published a paper where Fourier transforms were used to analyse beach sand silhouettes. In 1969 and 1970 Meloy [28, 29] presented papers in which fast Fourier transforms were used to process particle silhouette as a signal and this work was extended in 1977 [30, 31]. One of their main conclusions is that particles have 'signatures' which depend on A_n and not on θ_n and they propose the equation:

$$A_n = A_I \left(\frac{1}{n} \right)^S \quad (4.31)$$

A plot of $\log A_n$ against $\log n$ yields a straight line which has a slope S which depends on particle shape, rounder particles having lower slopes. Beddow [18] showed how a number of particle silhouette shapes could be analysed and reproduced by Fourier transforms. Gotoh and Finney [32] proposed a mathematical method for expressing a single, three-dimensional body by sectioning

as an equivalent ellipsoid having the same volume, surface area and average projected area as the original body.

4.2.6 Fractal dimension characterization of textured surfaces

Mandelbrot has introduced the term ‘fractal dimension’ to describe curves which have no unique perimeter. In his book [33] he describes how Richardson estimated the length of the coast line of various countries by stepping along a map of the coast line with a pair of dividers. He found that the estimated perimeter (P_λ) tends to increase without limit as the step size λ decreases. He concluded that a polygon of side n (n = number of steps) approximating a coast line would have $k\lambda^{-D}$ sides. The perimeter estimate would be:

$$P_\lambda = n\lambda \quad (4.32)$$

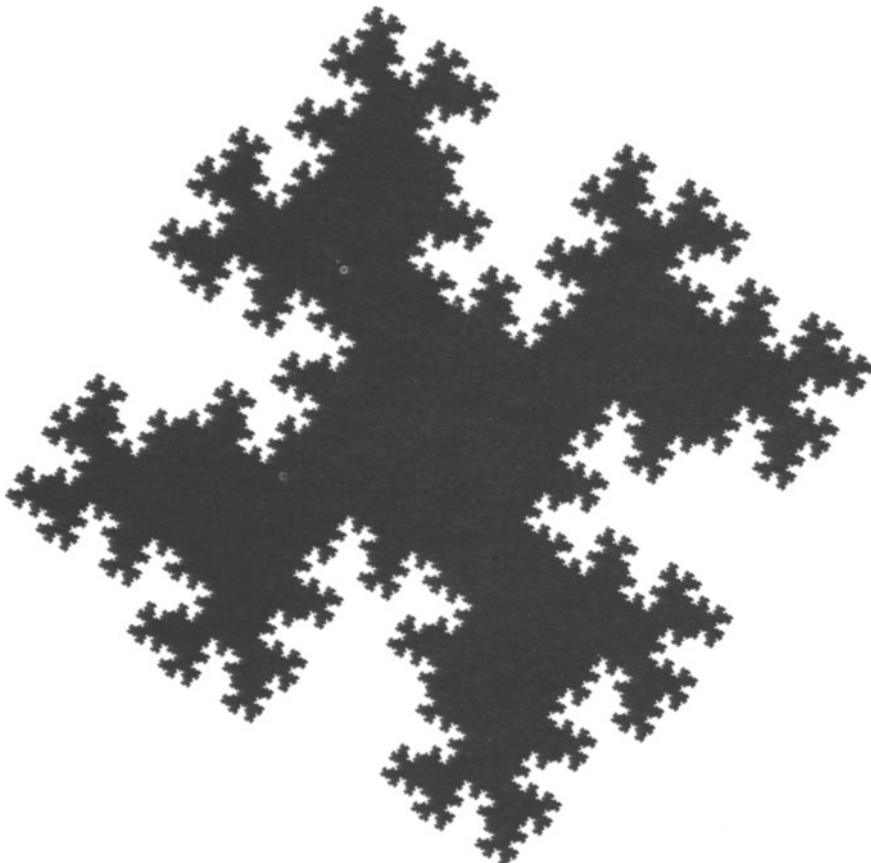


Figure 4.4 (a) A Triadic Koch Island.

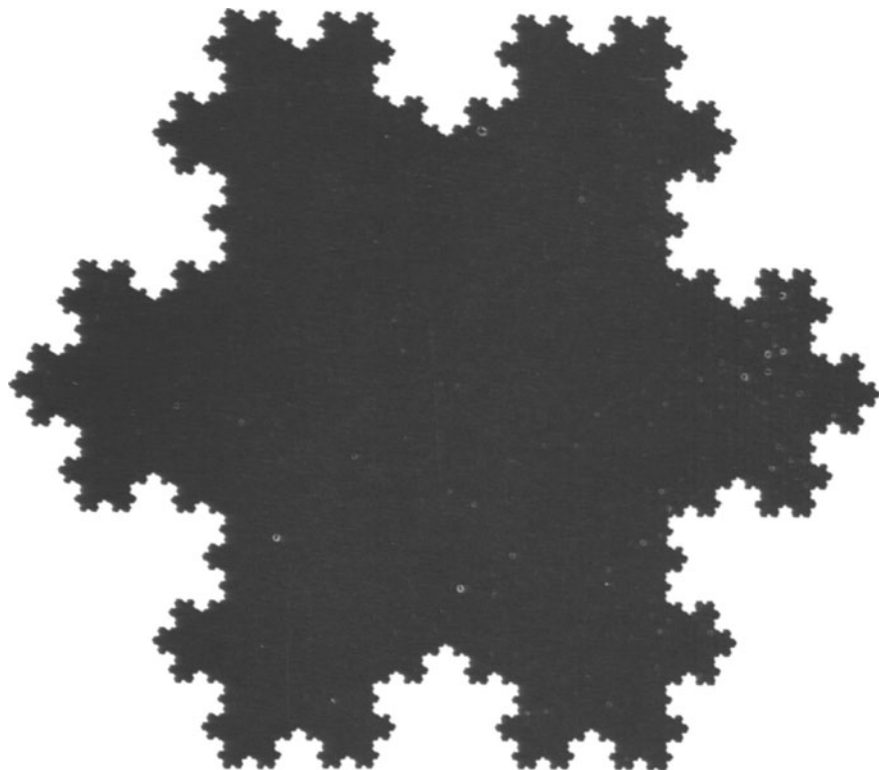


Figure 4.4 (b) A Quadric Koch Island [reproduced from 84].

$$P_\lambda = k\lambda^{1-D} \quad (4.33)$$

Hence a plot of $\log P_\lambda$ against $\log \lambda$ will have a slope $1 - D$. The parameter D was found to be characteristic of the particular coast line measured and was called by Mandelbrot the fractal.

Kaye [34] demonstrated that this technique could be applied to the determination of the ruggedness of carbon black agglomerates. Another procedure he utilized was to study the frequency of intersections made by the boundary of the profile with a grid placed at random under the profile using grids with a range of grid sizes. A third procedure he adopted was to determine the number of squares on the particle profile, accepting those that were largely inside the profile and rejecting others. The efficiencies of the three techniques were found to be in the order that they are presented above.

His main conclusion was that this technique was too time-consuming for manual operation and he recommended the use of image-analysing computers, a recommendation that was taken up by Flook [35] using a Quantimet 720. Flook considered the perimeter to be made up of a series of closely spaced

points. A series of circles of radius λ is drawn up with their centres on each of the points in turn thus describing a path of width 2λ covering the curve. The area of the path divided by its width gives an estimate of its length. The process is repeated with decreasing λ .

This method was applied to a circle which, being a Euclidean curve, has a fractal equal to unity. Two mathematical models examined consisted of geometrically constructed islands taken from Mandelbrot's book. The first was a Triadic Koch Island and the second a Quadric Koch Island (figure 4.4). Measurements were also made on a typical carbon black aggregate and a simulated carbon floc, taken from a paper by Medalia [36]. Excellent agreement was found between experimental and theoretical results.

4.3 DETERMINATION OF SPECIFIC SURFACE FROM SIZE DISTRIBUTION DATA

4.3.1 Number distribution

Let particles of size $d_{x,r}$ constitute a fraction m_r of the total number N so that:

$$\begin{aligned} m_r &= \frac{n_r}{N} \quad \text{and} \quad N = \sum n_r \\ S &= \alpha_{s,x} N \sum m_r d_{x,r}^2 \\ V &= \alpha_{v,x} N \sum m_r d_{x,r}^3 \\ S_v &= \alpha_{sv,x} \frac{\sum m_r d_{x,r}^2}{\sum m_r d_{x,r}^3} \end{aligned} \tag{4.34}$$

4.3.2 Surface distribution

Let particles of size $d_{x,r}$ constitute a fraction t_r of the total surface S so that:

$$\begin{aligned} t_r &= \frac{S_r}{S} \quad \text{and} \quad S = \sum S_r \\ St_r &= \alpha_{s,x} N m_r d_{x,r}^2 \\ V &= \frac{S}{\alpha_{sv,x}} \sum t_r d_{x,r} \\ S_v &= \frac{\alpha_{sv,x}}{\sum t_r d_{x,r}} \end{aligned} \tag{4.35}$$

4.3.3 Volume distribution

Let particles of size $d_{x,r}$ constitute a fraction q_r of the total volume V so that:

$$\begin{aligned} q_r &= \frac{V_r}{V} \quad \text{and} \quad V = \sum V_r \\ Vq_r &= \alpha_{v,x} N m_r d_{x,r}^3 \\ S_v &= \alpha_{sv,x} \sum \frac{q_r}{d_{x,r}} \end{aligned} \tag{4.36}$$

Equation (4.34) is used whenever a number count is taken and yields a specific surface if the shape coefficient is known and vice-versa. If α_{sv} is assumed equal to 6 (this is assuming spherical particles) a specific surface is obtained. For microscope counting by projected area this is written $S_{v,a}$.

Similar arguments apply to equations (4.35) and (4.36). The latter is frequently applied to sieve analyses where q_r is the fractional weight residing between two sieves of average aperture $d_{A,r}$.

4.4 PARTICLE SIZE DISTRIBUTION TRANSFORMATION BETWEEN NUMBER, SURFACE AND MASS

There are several methods of particle size measurement in which the raw data are collected in the form of a number distribution: microscopy, electrical and light-sensing zone methods are three widely used examples.

Transition is simple if one obtains a straight line on log-probability paper since the graphs for surface and weight are straight lines, parallel to the number distribution, but with the 50% value, corresponding to the surface mean x_{gs} and volume mean x_{gv} displaced (equations 4.129 and 4.135).

Considerable difficulties are presented if the log-normal law does not hold. The obvious way of calculating the proportion of surface or volume corresponding to particular particle diameters consists of weighting by the corresponding squared or cubed diameters [76]. The results are then summed to yield the cumulative surface or weight distribution. Conversion from number to surface or surface to volume is best carried out graphically, in order to smooth out experimental errors, as described in the section on photosedimentation. Nomograms have been developed to reduce the tedium and possible calculation errors involved in number to weight conversion [72, 73]. However, it is not in general likely that the conversion from number to weight will be accurate on the following grounds:

1. The weighted proportions are too sensitive to sample fluctuations since the method requires the raising of experimental errors to higher powers. (In a 1 to 10 µm distribution an error of one 10-µm particle has the same weighting as an error of a thousand 1-µm particles.)
2. The grouping of the observed diameters into frequency intervals, which in practice may be broad and non-uniform, makes an accurate estimation of the average for each size range impossible.

The mean diameter for each range is usually taken as the arithmetic mean $(\bar{x} = \frac{x_1 + x_2}{2})$ or less frequently the geometric mean $\bar{x} = \sqrt{x_1 x_2}$.

Thus, the fraction by weight of particles larger than D_r is given by:

$$W_r = \sum_{D_r}^{D_{\max}} D^3 dN \quad (4.37)$$

where $\sum_{D_{\min}}^{D_{\max}} D^3 dN = 1$, i.e. the distribution is normalized.

Integration by parts, however, yields the following equivalent relationship [74, 75]:

$$\begin{aligned} W_r &= D_r^3 N_r + 3 \sum_{D_r}^{D_{\max}} D^2 dN dD \\ &= D_r^3 N_r + 3 \left[(D_r^2 N_r + D_{r+1}^2 N_{r+1}) \left(\frac{D_{r+1} - D_r}{2} \right) \right. \\ &\quad \left. + (D_{r+1}^2 N_{r+1} + D_{r+2}^2 N_{r+2}) \left(\frac{D_{r+2} - D_{r+1}}{2} \right) + \dots \right] \end{aligned} \quad (4.38)$$

This is applied in Table 4.8 and the results are compared with weighting with cubed diameters.

In using this method the particle counts may be classified into fairly broad intervals thereby reducing experimental time. A computer program for carrying out this conversion has also been published [77]. The conversion is much more accurate, however, if the procedure laid down in the chapter on microscopy is followed. The errors are also reduced with electronic counting devices where the total count is large and the size intervals are small.

Conversion from weight to surface (e.g. sieving) may be carried out using the following expression:

$$\Delta S = \sum_{r-1}^{r+1} \frac{\Delta W_r}{d_{Ar}} \quad (4.39)$$

Table 4.8 Conversion from a number to a weight distribution

Particle size (D) (μm)	Cumulative number frequency oversize (N)	Cumulative weight frequency oversize ($W \div 5^3$)	Cumulative weight percentage oversize	$\Delta N \cdot D^{-2}$ ($\div 2.5$)	% ΣND^3
50 = D_m	0 = N_m	0 = W_m	0	.0	
45 = D_{m-1}	1 = N_{m-1}	850.5 = W_{m-1}	6.6	.6860	6.4
40	2	1459	11.3	.4913	11.0
35	3	1876.5	14.6	.3375	14.2
30 = D_r	7 = N_r	3021	23.6	.8788	22.4
25	16	4487	35.0	.11979	33.6
20	50	7487	58.4	.24786	56.7
15	112	10023	78.2	.21266	76.6
10	261	12165	95.0	.18625	94.0
5	380	12593	98.3	3213	97.0
1	400	12810	100.0	41	100.0

where ΔS is the relative surface of a weight of powder W_r residing between sieve sizes d_{Ar+1} and d_{Ar-1} .

$$(1) \quad W_m = 0$$

$$(2) \quad W_{m-1} = 45^3 \times 1 + 3 \left[(45^2 \times 1 + 0) \left(\frac{50 - 45}{2} \right) \right]$$

$$= 5^3 \left[9^3 \times 1 + 3(9^2 \times 1 + 0) \left(\frac{10 - 9}{2} \right) \right] = (729 + 121.5) \times 5^3$$

$$= 850.5 \times 5^3$$

$$(3) \quad W_{m-2} = 5^3 \left[8^3 \times 2 + 3(8^2 \times 2 + 9^2 \times 1) \left(\frac{9 - 8}{2} \right) \right]$$

$$= (1024 + 313.5 + 121.5) \times 5^3 = 1459 \times 5^3$$

and so on.

4.5 AVERAGE DIAMETERS

The purpose of an average is to represent a group of individual values in a simple and concise manner in order to obtain an understanding of the group. It is important, therefore, that the average should be representative of the group. All average diameters are a measure of central tendency which is

Table 4.9 Cumulative percentage undersize distribution

Particle size (μm)	Cumulative percentage undersize
x_2	$\phi = \sum_0^x d\phi$
5	1.4
9	9.4
11	18.0
14	32.0
17	49.5
20	64.0
23	76.0
28	88.0
33	94.0
41	98.0
50	99.4
60	99.9

ϕ , the frequency function = ΣdN for a number distribution
= $\Sigma x dN$ for a size distribution
= $\Sigma x^2 dN$ for an area distribution
= $\Sigma x^3 dN$ for a volume or weight distribution
where dN is the percentage of the total
number of particles lying in the size range
 x_1 to x_2 .

unaffected by the relatively few extreme values in the tails of the distribution. Some of these are illustrated in Tables 4.9 and 4.10 and figures 4.5 and 4.6.

The most commonly occurring value, the mode, passes through the peak of the relative frequency curve, i.e. it is the value at which the frequency density is a maximum. The median line divides the area under the curve into equal parts, i.e. it is the 50% size on the cumulative frequency curve. The vertical line at the mean passes through the centre of gravity of a sheet of uniform thickness and density cut to the shape of the distribution. Hence, for the mean, the moment of the sum of all the elementary areas of thickness δx about the ordinate equals the sum of all the moments:

$$\bar{x} \sum \frac{d\phi}{dx} \delta x = \sum x \frac{d\phi}{dx} \delta x$$

$$\bar{x} = \frac{\sum x d\phi}{\sum d\phi} \quad (4.40)$$

For a weight distribution $d\phi = x^3 dN$ giving:

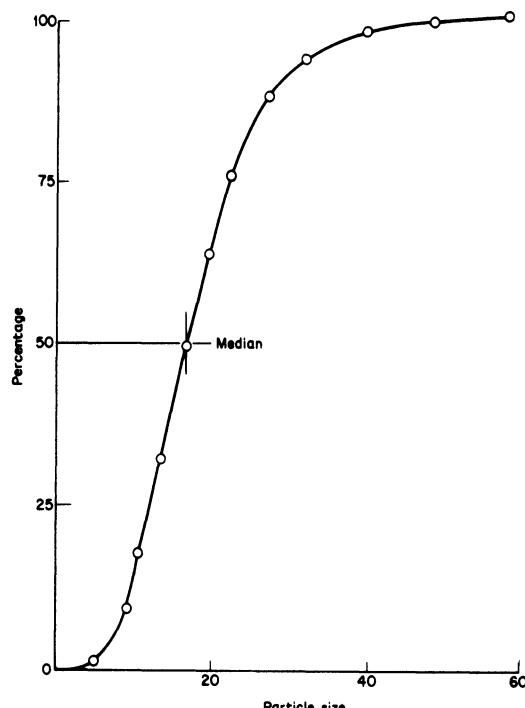


Figure 4.5 The cumulative percentage frequency curve.

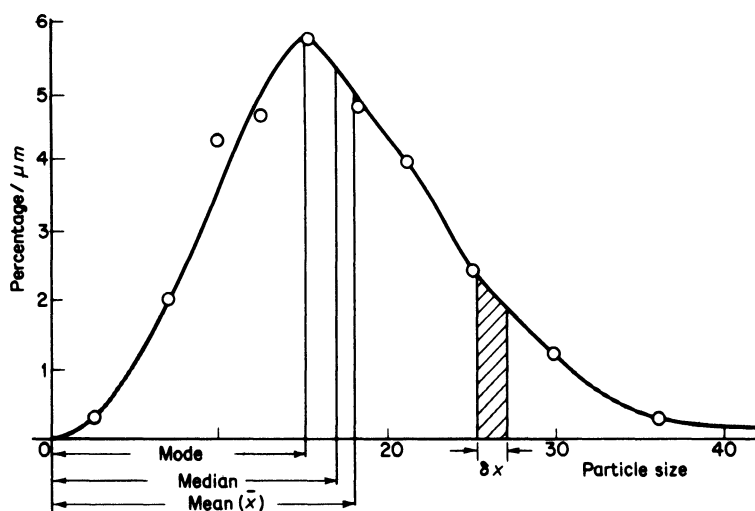


Figure 4.6 The relative percentage frequency curve.

$$\bar{x} = \frac{\sum x^4 dN}{\sum x^3 dN} \quad (4.41)$$

The mode and the median may be determined graphically but the above summation has to be carried out for the determination of the mean. However, for a slightly skewed distribution, the approximate relationship $\text{mean} - \text{mode} = 3(\text{mean} - \text{median})$ holds. For a symmetrical distribution, they all coincide. In the illustration, the values are: mode = 15.0; median = 17.2; yielding mean = 18.2, as compared with the summed value of 18.47 (see Table 4.10).

Table 4.10 Relative percentage frequency distribution: tabular calculation of mean size

Particle size range x_1 to x_2	Interval dx	Average size x	Percentage in range $d\phi$	Percentage per micrometre $d\phi/dx$	$xd\phi$
0 to 5	5	2.5	1.4	0.3	4
5 to 9	4	7.0	8.0	2.0	56
9 to 11	2	10.0	8.6	4.3	86
11 to 14	3	12.5	14.0	4.7	175
14 to 17	3	15.5	17.5	5.8	271
17 to 20	3	18.5	14.5	4.8	268
20 to 23	3	21.5	12.0	4.0	258
23 to 28	5	25.5	12.0	2.4	306
28 to 33	5	30.5	6.0	1.2	183
33 to 41	8	37.0	4.0	0.5	148
41 to 50	9	45.5	1.4	0.2	64
50 to 60	10	55.0	0.5	0.1	28
$\Sigma x d\phi$					1847
Mean size = $\frac{\Sigma x d\phi}{\Sigma d\phi}$					18.47

The characteristics of a particle distribution are its total number, length, area and volume. A system of unequally sized particles may be represented by a system of uniformly sized particles having two, and only two, characteristics of the original distribution. The size of the particles in the uniform system is then the mean size of the non-uniform system with respect to these two properties.

The sizes may be expressed mathematically by dividing the system of particles into small intervals of size δx with assumed diameters of x_1, x_2, \dots . The symbol x is used because the method of measurement for individual particles is not specified, and all particles are assumed to have the same shape. Let the

numbers of particles in these groupings be $\delta N_1, \delta N_2 \dots$ respectively. Then the aggregate length, surface and volume of the particles in each grouping are $x\delta N$, $x^2\delta N$ and $x^3\delta N$ and the total for the system is the summation of these expressions. Table 4.11 is a summary of the mathematical expressions for the various mean diameters [3].

The method of sizing may also be incorporated into the symbol. Hence, for particle sizing by microscopy, the arithmetic mean diameter becomes $d_{a,NL}$. The surface-volume diameter calculated from the results of a sedimentation experiment is $d_{St,sv}$. The mean value of a cumulative weight percentage curve obtained by sieving would be $d_{A,vm}$ or $d_{A,wm}$.

Table 4.11 Definitions of mean diameters

Number, length mean diameter	$x_{NL} = \frac{\sum dL}{\sum dN} = \frac{\sum x dN}{\sum dN}$
Number, surface mean diameter	$x_{NS} = \sqrt{\left(\frac{\sum dS}{\sum dN}\right)} = \sqrt{\left(\frac{\sum x^2 dN}{\sum dN}\right)}$
Number, volume mean diameter	$x_{NV} = \sqrt[3]{\left(\frac{\sum dV}{\sum dN}\right)} = \sqrt[3]{\left(\frac{\sum x^3 dN}{\sum dN}\right)}$
Length, surface mean diameter	$x_{LS} = \frac{\sum dS}{\sum dL} = \frac{\sum x^2 dN}{\sum x dN}$
Length, volume mean diameter	$x_{LV} = \sqrt{\left(\frac{\sum dV}{\sum dL}\right)} = \sqrt{\left(\frac{\sum x^3 dN}{\sum x dN}\right)}$
Surface, volume mean diameter	$x_{SV} = \frac{\sum dV}{\sum dS} = \frac{\sum x^3 dN}{\sum x^2 dN}$
Volume, moment mean diameter	$x_{VM} = \frac{\sum dM}{\sum dV} \frac{\sum x^4 dN}{\sum x^3 dN}$
Weight, moment mean diameter	$x_{WM} = \frac{\sum dM}{\sum dW} = \frac{\sum x dW}{\sum dW} = \frac{\sum x^4 dN}{\sum x^3 dN}$

Consider the system illustrated (figure 4.7) consisting of one particle of size 1, 2, 3, 4, 5, 6, 7, 8, 9, 10. Hence ten particles, each of length 5.50, will have the same total length as the original distribution (Table 4.12). Similarly ten particles, each of length 6.21, will have the same total surface as the original distribution.

Each of these mean diameters characterizes the original distribution in two properties only. For example, the length-surface mean diameter is 7.00. Therefore, the uniform system contains $N = (L/x) = (S/x^2)$, which is 7.87 in each case. Hence, the uniform system consists of 7.87 particles, each of length 7.00. Thus, the total length and the total surface of the particles are the same

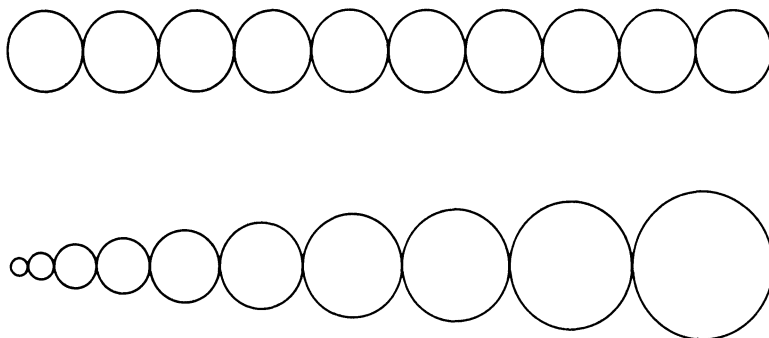


Figure 4.7 The homogeneous distribution that represents in number and length a heterogeneous distribution of ten particles of size 1 to 10 with unit separation in size.

as in the original distribution, but the total number, volume and moment are all different, e.g. $V = x^3N = 343 \times 7.87 = 2700$.

Table 4.12

$x_{NL} = 5.50$	$x_{LS} = 7.00$	$x_{VM} = 8.37$	$\Sigma dV = 3025$
$x_{NS} = 6.21$	$x_{LV} = 7.43$	$\Sigma dL = 55$	$\Sigma dM = 25335$
$x_{NV} = 6.71$	$x_{SV} = 7.87$	$\Sigma dS = 385$	

The arithmetic mean is the sum of the diameters of the separate particles divided by the number of particles, it is most significant when the distribution is normal:

$$x_A = x_{NL} = \frac{\sum x dN}{\sum dN} \quad (4.42)$$

The geometric mean is the n th root of the product of the diameters of the n particles examined; it is of particular value with log-normal distributions:

$$x_g = (\prod x^{dN})^{1/N} \quad (4.43)$$

$$N \log x_g = \sum dN \log x$$

$$\log x_g = \frac{\sum dN \log x}{N} \quad (4.44)$$

The harmonic mean is the number of particles divided by the sum of the reciprocals of the diameters of the individual particles; this is related to specific surface and is of importance where surface area of the sample is concerned [37].

$$x_H = \frac{\Sigma dN}{\Sigma dN/x} \quad (4.45)$$

4.6 PARTICLE DISPERSION

The spread of the distribution data may be expressed in terms of the *range*, i.e. the difference between the minimum and maximum sizes; the interquartile range ($_{25}x_{75}$), i.e. the difference between the 75% and 25% sizes; an interpercentile range, e.g. ($_{20}x_{80}$), the difference between the 80% and 20% sizes or the standard deviation.

The least significant of these is the first, since a stray oversize or undersize particle can greatly affect its value. The most significant is the last, since every particle has a weighting which depends on the difference between its size and the mean size.

The standard deviation (σ) is defined as:

$$\sigma = \sqrt{\left(\frac{\sum (x - \bar{x})^2 \Delta \phi}{\sum \Delta \phi} \right)} \quad (4.46)$$

Hence:

$$\sigma^2 = \frac{\sum x^2 \Delta \phi}{\phi} - \bar{x}^2 \quad (4.47)$$

where σ^2 is called the variation.

4.7 METHODS OF PRESENTING SIZE ANALYSIS DATA

An example of the tabular method of presenting size distribution data is shown in Table 4.13. The significance of the distribution is more easily grasped when the data are presented pictorially, the simplest form of which is the histogram. The data in Table 4.13 give the size grading of 1000 particles in 12 class intervals which are in a geometric progression. The choice of class widths is of fundamental importance, the basic requirement being that the resolution defined as the class interval divided by the mean class size should be kept fairly constant. With narrowly classified powders, an arithmetic distribution is acceptable but it is more normal to use a geometric progression.

Consider an analysis of a sub-sieve powder. For an arithmetic progression of sizes, let the intervals be 2.5 to 7.5, 7.5 to 12.5, and so on, to 67.5 to 72.5 μm . The resolution will then vary from 1 to 0.071 as the particle size increases. A geometric progression with the same number of size intervals is 0.14 to 1.18, 1.18 to 1.68, 1.68 to 2.36, and so on, to 53.7 to 75.5 with

Table 4.13 Size data

Particle size range	Interval	Average size	Number frequency in range	Percentage in range	Percentage per micron	$\frac{d\phi}{dx}$	$\frac{d\phi}{d \log x}$
x_2 to x_1	dx	x	dN	$d\phi$			
1.4 to 2.0	0.6	1.7	1	0.1	0.2	1	
2.0 to 2.8	0.8	2.4	4	0.4	0.5	3	
2.8 to 4.0	1.2	3.4	22	2.2	1.8	15	
4.0 to 5.6	1.6	4.8	69	6.9	4.3	46	
5.6 to 8.0	2.4	6.8	134	13.4	5.6	89	
8.0 to 11.2	3.2	9.6	249	24.9	7.8	167	
11.2 to 16.0	4.8	13.6	259	25.9	5.4	173	
16.0 to 22.4	6.4	19.2	160	16.0	2.5	107	
22.4 to 32.0	9.6	27.2	73	7.3	0.8	49	
32.0 to 44.8	12.8	38.4	21	2.1	0.2	14	
44.8 to 64.0	19.2	54.4	6	0.6	0.0	4	
64.0 to 89.6	25.6	76.8	2	0.2	—	1	
$N = 1000$							

$$\text{where } y = \frac{d\phi}{dx} \text{ and } d\phi = 100 \frac{dN}{N}$$

geometric means of 1, $\sqrt{2}$, $2\sqrt{2}$, 4 to 64. The resolution for each size range is constant at 0.34. If there is a constant error in defining the class intervals, say, a 1 μm undersizing, the effect of this error will be dependent on the size with an arithmetic progression being greater for small particles, whereas with a geometric size interval, the effect is independent of particle size.

Three methods of presenting the histogram are available. In the first, a rectangle is constructed over each class interval, the height of which is proportional to the number of particles in that interval (figure 4.8).

A far more useful way is to construct rectangles whose areas are proportional to the numbers of particles in the intervals. The total area under the histogram is equal to the number of particles counted, and it is useful to reduce this number to 100 by making the areas under the rectangles equal to the percentages of particles in the intervals so that histograms may be compared irrespective of the number of particles counted (figure 4.9).

If a sufficient number of particles has been counted, a smooth curve may be drawn through the histogram to give a frequency distribution. It is usual to have more than twelve intervals for this reason, with an upper limit of about twenty in order that the number of particles in each interval remains high and the work involved does not become too great.

It is often more convenient to plot the information as a cumulative dis-

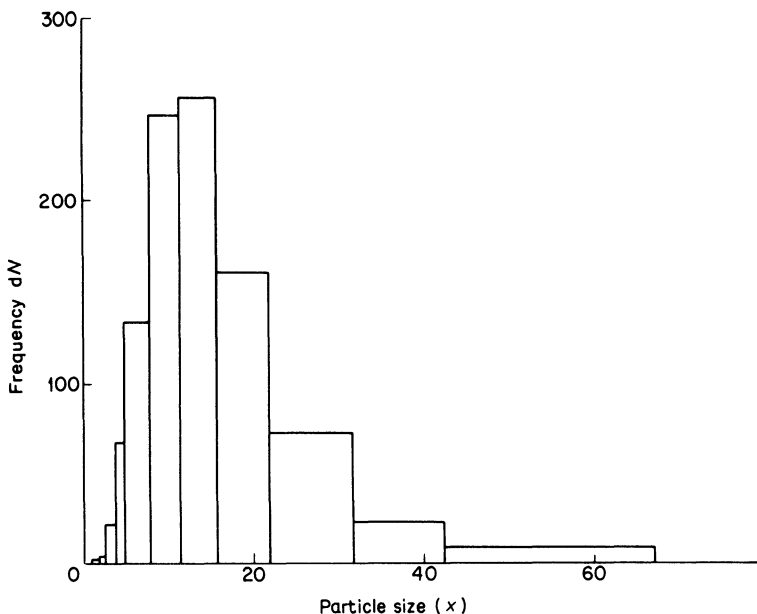


Figure 4.8 Number-frequency histogram.

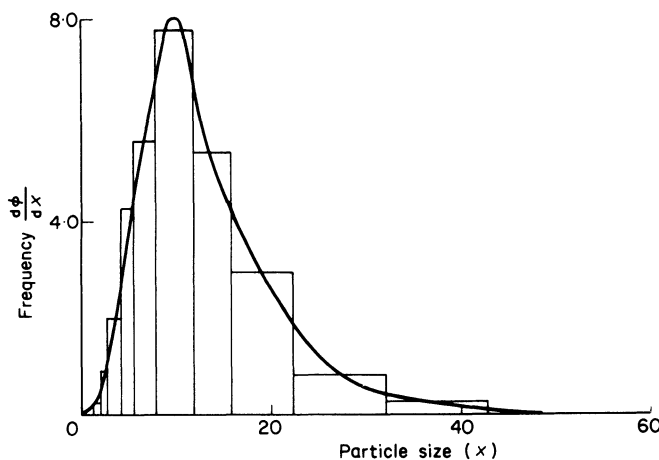


Figure 4.9 The relative percentage frequency distribution by number.

tribution; the abscissa is particle size and the ordinate, the percentage smaller than or larger than the size. This method has the advantage that the median size and the percentage between any two sizes may be read off directly. The cumulative curve does often conceal detail and for comparison of similar size gradings, the relative percentage frequency should be used. If the range of particle size is very great, particularly if the intervals are in a geometric

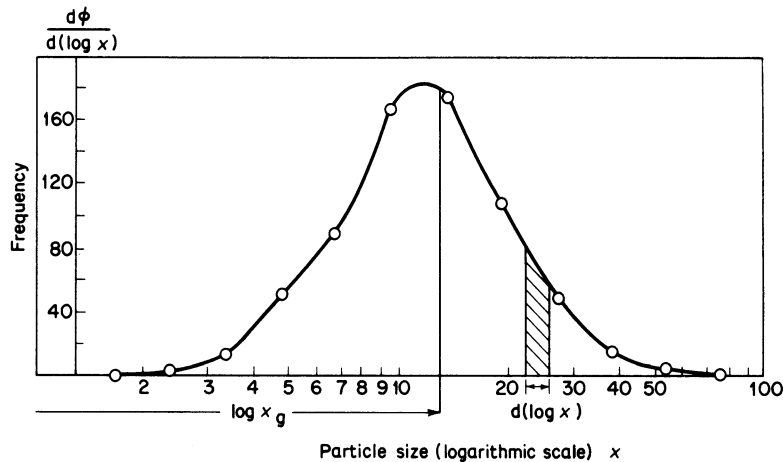


Figure 4.10 A log-normal distribution plotted as a relative percentage frequency distribution using a logarithmic scale for particle size.

progression, it is advisable to use a logarithmic scale. In order that the distribution be plotted according to an equidistant log scale $x(d\phi/dx)$ is plotted against $\ln x$ instead of $d\phi/dx$ against x as with the distribution curve using a linear abscissa [38, p. 90]. Alternatively, $d\phi/d \log x$ may be plotted against $\log x$ (figure 4.10).

The mean size in this case is the geometric mean given by:

$$\log x_g \sum \frac{d\phi}{d \log x} \cdot d \log x = \sum \log x \frac{d\phi}{d \log x} \cdot d \log x$$

$$\log x_g = \frac{\sum \log x d\phi}{\sum d\phi} \quad (4.48)$$

(cf. equation (4.40)). ϕ is a general term for the variables W , S and N , i.e. weight, surface and number.

4.8 DEVICES FOR REPRESENTING THE CUMULATIVE DISTRIBUTION CURVE AS A STRAIGHT LINE

4.8.1 Arithmetic normal distributions

It is common practice to plot size distribution data in such a way that a straight line results, with all the advantages that follow from such a reduction. This can be done if the distribution fits a standard law, such as the normal law. This distribution occurs when the measured value of some property of a

system is determined by a large number of small effects, each of which may or may not operate. If a large number of the measurements of the value are made, and the results plotted as a frequency distribution, the well-known, bell-shaped curve results.

Although it might be expected that this type of distribution would be common, it seems to occur only for narrow size ranges of classified material. Actual distributions are skewed, usually to the right.

The equation representing the normal distribution is:

$$y = \frac{1}{\sigma\sqrt{2\pi}} \exp\left[-\frac{(x - \bar{x})^2}{2\sigma^2}\right] \quad (4.49)$$

where $y = \frac{d\phi}{dx} = f(x)$

and $\int_{-\infty}^{\infty} f(x)dx = 1$ (i.e. the distribution is normalized),

σ is the standard deviation (σ^2 is the variance), \bar{x} is the mean size and ϕ is a general term for the frequency, being number, length, surface or volume.

$$\text{Let } t = \left(\frac{x - \bar{x}}{\sigma}\right)$$

then $\sigma dt = dx$.

Equation (4.49) becomes:

$$\frac{d\phi}{dt} = \frac{1}{\sqrt{2\pi}} \exp\left(-\frac{t^2}{2}\right)$$

$$\text{Hence: } \int_0^\phi d\phi = \frac{1}{\sqrt{2\pi}} \int_{-\infty}^x \exp\left(-\frac{t^2}{2}\right)^2 dt \quad (4.50)$$

A plot of $\frac{d\phi}{dt}$ against t results in the well-known ‘dumb-bell’ shape of the normal probability curve (figure 4.11).

Equation (4.50) is the basis for arithmetic probability graph paper and the integral is tabulated in books on statistics (Table 4.14).

The integral from Table 4.14, for $t = 1$ is 84.13%, or for $t = -1$ is 15.8%; therefore, the standard deviation:

$$\sigma = \left(\frac{x - \bar{x}}{t}\right) = x_{84.13} - x_{50} = x_{50} - x_{15.87}$$

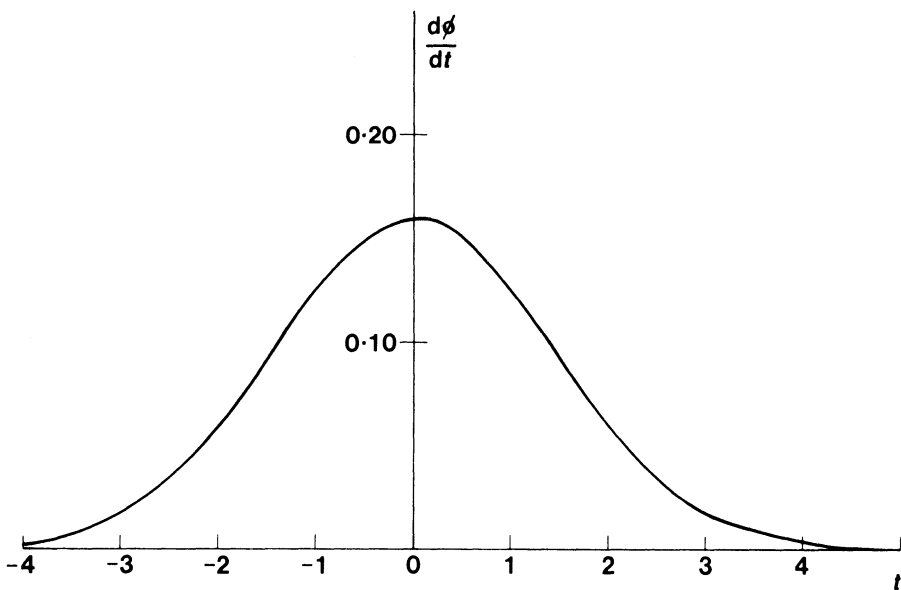


Figure 4.11 The normal probability curve. Relative frequency against standard deviation [68.26% of the distribution lies within 1 standard deviation $-1 < t < +1$ of the mean].

Table 4.14 Integration of the normal probability equation

t	Integral
0	0.5000
0.5	0.6915
1.0	0.8413
1.5	0.9332
2	0.9772
3	0.9987
4	0.99997

A powder whose size distribution fits the normal equation can therefore be represented by two numbers, the mean value and the standard deviation. The fraction of particles lying between given sizes can then be found from the tables giving the areas under the graph between any two ordinates; such tables are published in Herdan's book [38, p. 77]. One advantage of this method of plotting is that experimental and operator errors may be smoothed out and the median and standard deviation can be read off the graph. In the illustrated example (figure 4.12), the median size, i.e. the 50% size, is 35 µm, and the standard deviation is half the difference between the 84% and the 16% sizes (15 µm):

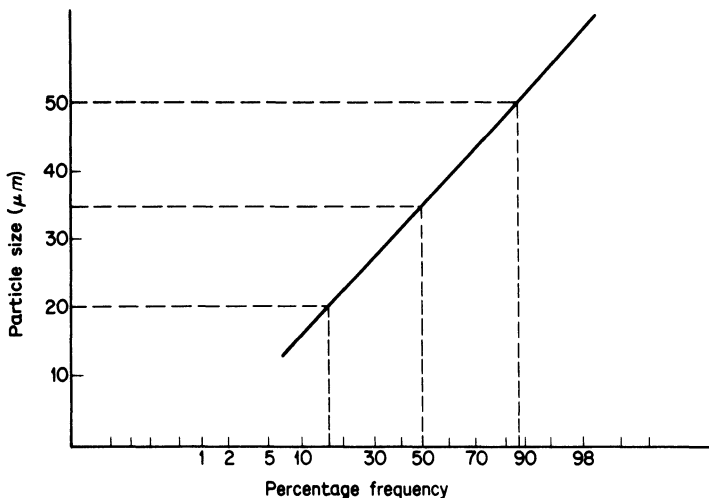


Figure 4.12 A normal distribution plotted on normal probability paper.

It can be seen from the graph (figure 4.12) that a 1% unit around 95% probability is of about four times the size range as that around the 50% probability. This tends to aggravate the errors discussed under the theory of compensating errors, hence it is usual to draw a best straight line through the central points.

If all particles greater or smaller than a certain particle size have been removed, the curve becomes asymptotic towards these sizes. It is also possible to determine whether the distributions are homogeneous or heterogeneous since, in the latter case, points of inflection occur. These and other cases are discussed in detail by Irani and Callis [39, p. 47].

4.8.2 The log-normal distribution

According to the normal law, it is differences of equal amounts in excess or deficit from a mean value which are equally likely. With the log-normal law, it is ratios of equal amounts which are equally likely. In order to obtain a symmetrical curve of the same shape as the normal curve, it is therefore necessary to plot the relative frequency against log size (see figure 4.10).

The equation of the log-normal distribution is obtained by replacing x with $z = \ln x$, in equation (4.49). Then:

$$y = \frac{1}{\sigma_z \sqrt{2\pi}} \exp \left[-\frac{(z - \bar{z})^2}{2\sigma_z^2} \right] \quad (4.51)$$

where $y = \frac{d\phi}{d \ln x}$, σ_z is the standard deviation of z

and $\bar{z} = \frac{\sum z d\phi}{\sum d\phi}$ ($\phi = N, S$ or W)

$$\bar{z} = \frac{\sum z d\phi}{\phi}$$

or $\ln x_g = \frac{\sum \ln x d\phi}{\phi}$

Therefore $x_g = [\sqrt{\prod x^{d\phi}}]^{1/\phi}$ (4.52)

$\prod x^{d\phi}$ is the product of the group data in which the frequency of particles of size x is $d\phi$, that is, the mean of a log-normal distribution is the geometric mean, i.e. the arithmetic mean of the logarithms:

$$x_g^\phi = x_1^{d\phi_1} x_2^{d\phi_2} \dots x_r^{d\phi_r} \dots x_n^{d\phi_n}$$

Since the particle size is plotted on a logarithmic scale, the presentation of data on a log-probability graph is particularly useful when the range of sizes is large.

As before, the median particle size of the data presented on the graph (figure 4.13) is the 50% median size ($20 \mu\text{m}$) and this is equal to the geometric mean size x_g . The geometric standard deviation is:

$$\begin{aligned}\log \sigma_g &= \log x_{84} - \log x_{50} \\ &= \log x_{50} - \log x_{16}\end{aligned}$$

or $2 \log \sigma_g = \log x_{84} - \log x_{16}$

$$= \log \frac{x_{84}}{x_{16}} \quad (4.53)$$

From figure 4.13

$$\begin{aligned}\log \sigma_g &= \frac{1}{2} \log \frac{40}{10} \\ &= \log 2\end{aligned}$$

Therefore:

$$\sigma_g = 2.$$

As a rule, if the number distribution of a given variable obeys a certain distribution law, the weight distribution does not and vice versa. This is not true for the log-normal distribution. If the number distribution is log-normal,

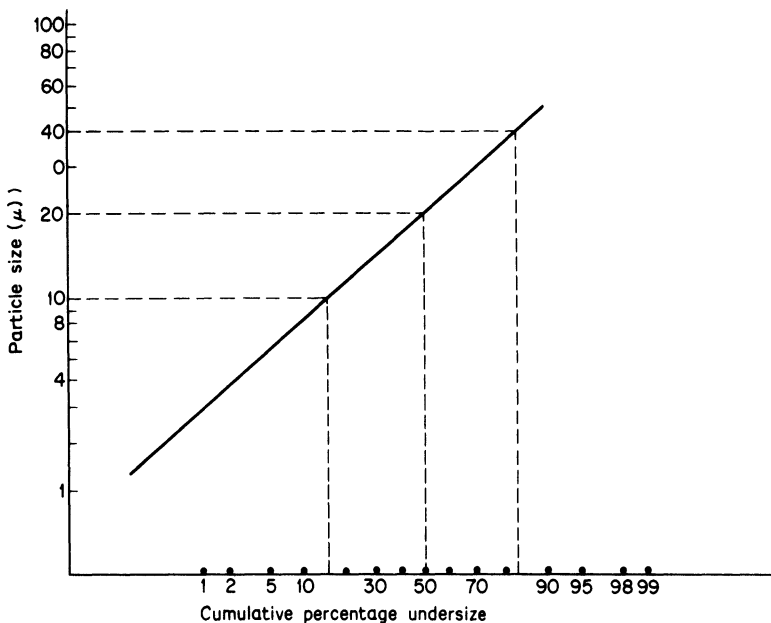


Figure 4.13 A log-normal distribution plotted on log-probability paper.

the surface and weight distributions are also log-normal with the same standard deviation [38, p. 85]. Conversion from one distribution to another is easy using the following equations (see section 4.12).

- (a) $\ln x_{NL} = \ln x_{gN} + 0.5 \ln^2 \sigma_g$
- (b) $\ln x_{NS} = \ln x_{gN} + 1.0 \ln^2 \sigma_g$
- (c) $\ln x_{NV} = \ln x_{gN} + 1.5 \ln^2 \sigma_g$
- (d) $\ln x_{NM} = \ln x_{gN} + 2.0 \ln^2 \sigma_g$ (4.54)

where x_{gN} is the geometric mean (median) of the number distribution and:

$$x_{NL} = \frac{\Sigma x dN}{\Sigma dN}; x_{NS}^2 = \frac{\Sigma x^2 dN}{\Sigma dN}; x_{NV}^3 = \frac{\Sigma x^3 dN}{\Sigma dN}; x_{NM}^4 = \frac{\Sigma x^4 dN}{\Sigma dN}$$

Derived sizes are obtained in the following manner:

$$\begin{aligned} \text{Surface-volume } x_{sv} &= \frac{\Sigma x^3 dN}{\Sigma x^2 dN} \\ &= x_{NV}^3 / x_{NS}^2 \end{aligned}$$

$$\begin{aligned} \text{Therefore: } \ln x_{sv} &= 3 \ln x_{NV} = 2 \ln x_{NS} \\ &= \ln x_{gN} + 2.5 \ln^2 \sigma_g \end{aligned} \quad (4.55)$$

If the initial analysis was a weight analysis, the above equations may be utilized using the conversions:

- $\ln x_{gS} = \ln x_{gN} + 2 \ln^2 \sigma_g$
- $\ln x_{gV} = \ln x_{gN} + 3 \ln^2 \sigma_g$ (4.56)

where x_{gN} , x_{gS} and x_{gV} are the number, surface and volume geometric mean diameters.

Table 4.15 Log-normal distribution

Particle size range (μm)	Average size (x)	$\log x$	Cumulative % oversize ϕ	Percentage in range $d\phi$	$\frac{d\phi}{d \log x}$	$\log x \, d\phi$
$\sqrt{2}-2$	1.68	0.225	0.4	0.4	2.7	0.09
$2-2\sqrt{2}$	2.38	0.376	3.5	3.1	20.5	1.17
$2\sqrt{2}-4$	3.36	0.526	14.5	11.0	72.8	5.79
$4-4\sqrt{2}$	5.76	0.677	36.3	21.8	144.2	14.77
$4\sqrt{2}-8$	6.72	0.827	63.6	27.3	180.8	22.58
$8-8\sqrt{2}$	9.52	0.978	85.6	22.0	145.7	21.52
$8\sqrt{2}-16$	13.4	1.029	95.7	10.1	66.9	10.40
$16-16\sqrt{2}$	19.0	1.179	99.6	3.9	25.8	4.60
$16\sqrt{2}-32$	26.9	1.430	100.0	0.4	2.7	0.57
						81.49

Assuming a weight distribution ($d\phi = dW = x^3 dN$):

$$\begin{aligned}\log x_{gV} &= \frac{\sum \log x d\phi}{d\phi} \\ &= 0.815 \\ x_{gV} &= 6.53 \mu\text{m}\end{aligned}$$

σ_g may also be obtained from the table, but both these values may be obtained more readily from a graph giving:

$$\begin{aligned}x_{gV} &= x_{\text{median}} = 6.6 \mu\text{m} \\ \sigma_g &= 1.64 (\log \sigma_g = 0.215)\end{aligned}$$

The number distribution will have a median:

$$\begin{aligned}\log x_{gN} &= \log x_{gV} - 6.9 \log^2 \sigma_g \\ &= 0.815 - 6.9 \times 0.215^2\end{aligned}$$

$$x_{gN} = 3.28 \mu\text{m}$$

Similarly: $\log x_{gS} = \log x_{gV} - 2.3 \log^2 \sigma_g$

$$x_{gS} = 5.11 \mu\text{m}$$

Mode: $\ln x_m = \ln x_{gV} - \ln^2 \sigma_g$

$$x_m = 5.11.$$

In each case the slope of the log-normal line, hence the standard deviation σ_g , will be the same; from equations (4.54):

$$X_{LS} = 3.67$$

$$X_{VS} = 4.10$$

$$X_{VM} = 4.55$$

$$X_{NL} = 3.30$$

$$X_{NS} = 3.48$$

$$X_{NM} = 3.87$$

4.8.3 The Rosin–Rammler distribution

For broken coal, a distribution function has been developed which has since been found to apply to many other materials [40]. For example, the particle size distribution of moon dust is found to closely follow a Rosin–Rammler distribution, hence it is assumed that the lunar surface was formed as a result of crushing forces due to impact [78].

Let the size distribution of broken coal be obtained by sieving and let the weight percentage retained on the sieve of aperture x be denoted by R ; a plot of R against x gives the cumulative percentage oversize curve.

From the probability considerations the authors obtain:

$$\frac{dF(x)}{dx} = 100nbx^{n-1} \exp(-bx^n) \quad (4.57)$$

where n and b are constants, b being a measure of the range of particle size present and n being characteristic of the substance being analysed. Integrating gives:

$$R = 100 \exp(-bx^n) \quad (4.58)$$

This reduces to: $\log \log \frac{100}{R} = \text{constant} + n \log x$ (4.59)

If log-log $100/R$ is plotted against $\log x$, a straight line results. The peak of the distribution curve for $n = 1$ is at $100/e = 36.8\%$, and denoting the mode of the distribution curve by x_m equation (4.58) gives $b = 1/x_m$.

The sieve opening for $R = 36.8\%$ is used to characterize the degree of comminution of the material, and since the slope of the line on the Rosin–Rammler graph depends on the particle size range, the ratio of $\tan^{-1}(n)$ and x_m is a form of variance.

This treatment is useful for monitoring grinding operations for highly skewed distributions, but should be used with caution since the device of taking logs always reduces scatter, hence taking logs twice is not to be recommended.

4.8.4 Mean particle sizes and specific surface evaluation for Rosin–Rammler distributions

The moment-volume mean diameter is given by:

$$x_{vm} = \frac{\sum x \Delta W}{\sum \Delta W} \quad (4.60)$$

Since $\Delta W = \Delta F(x)$, defining $F(x)$ as 100 gives from equations (4.57) and (4.60):

$$\begin{aligned} x_{vm} &= \frac{1}{100} \int_0^{\infty} 100nb x^n \exp(-bx^n) dx \\ &= \frac{1}{n\sqrt{b}} \Gamma\left(\frac{1}{n} + 1\right) \end{aligned}$$

The surface-volume mean diameter may be similarly evaluated as:

$$x_{sv} = \frac{1}{n\sqrt{b}\Gamma(1 - \frac{1}{n})}, n > 1$$

These can be evaluated from tables of gamma functions for experimental values of n and the specific surface determined.

4.8.5 Other particle size distribution equations

Various other size distribution functions have been proposed. These are usually in the form of two-parameter (b and n) potential distribution functions such as:

- (a) Gates–Gaudin–Schumann [60, 61]

$$\phi_{GGS} = (bx)^n \quad (4.61)$$

(b) Gaudin-Meloy [62]

$$\phi_{GM} = [1 - (1 - bx)^n] \quad (4.62)$$

where ϕ is the undersize fraction.

Three- and four-parameter functions with more accuracy have also been proposed [63–65].

4.8.6 Simplification of two-parameter equations

Tarjan [66] converted a two-parameter size distribution function from the form $\phi = f(x)$ to the form $\phi = f(x/x_{0.5})$ where $x_{0.5}$ is the median size. This results in an easy-to-handle function with a high degree of correspondence to the more complicated logarithmic function (ϕ_K) below [67].

$$\phi_K = \Phi \ln(bx)^n \quad (4.63)$$

where

$$\Phi = \frac{1}{\sqrt{2\pi}} \int_{-\infty}^u \exp\left(-\frac{u^2}{2}\right) \cdot du \quad (4.64)$$

Let the parameter b of equations (4.58), (4.61), (4.62) and (4.63) be expressed in terms of $x_{0.5}$ when $\phi = 0.50$ ($R = 50$ in equation (4.55)).

$$GGS: \quad 0.50 = (bx_{0.5})^n$$

$$RR: \quad 0.50 = \exp(-bx_{0.5}^n)$$

$$GM: \quad 0.50 = (1 - bx_{0.5})^n$$

Substituting back for b gives:
equation (4.58)

$$\phi_{RR} = 1 - \exp\left[-\left(\frac{x}{x_{0.5}}\right)^n \ln 2\right] \quad (4.65)$$

equation (4.61)

$$\phi_{GGS} = 0.5 \left(\frac{x}{x_{0.5}}\right)^n \quad (4.66)$$

equation (4.62)

$$\phi_{GM} = 1 - \left[1 - \left(\frac{x}{x_{0.5}}\right)(1 - \sqrt[3]{0.5})\right]^n \quad (4.67)$$

4.8.7 Evaluation of non-linear distributions on log-normal paper

A bimodal distribution is detectable on log-probability paper by a change in slope of the line. It is also possible to deduce further features of the distribution. Figure 4.14 shows a bimodal distribution in which the parent distributions do not intersect on a log-probability plot. These distributions are asymptotic to the parent distributions. The geometric means of the parent distributions may be obtained by plotting relative percentage frequency against particle size on log-linear paper (figure 4.15). The area under the two quite distinct curves gives the proportions of the two constituents. From the modes to the 34% levels in areas gives the two standard deviations.

Figure 4.16 shows a bimodal distribution in which the parent distributions intersect on a log-probability plot. These distributions are asymptotic to the parent distribution having the widest size range (i.e. high standard deviation). The point of inflection passes through both distributions. If the separation of means is large, these may be obtained from a plot of relative percentage frequency against particle size on log-linear paper. If the separation of means is small, it is difficult to resolve these distributions (figure 4.17).

Figure 4.18 shows a trimodal distribution. This may also be easily resolved into its component parts if the parent distributions do not intersect on log-probability paper (figure 4.19).

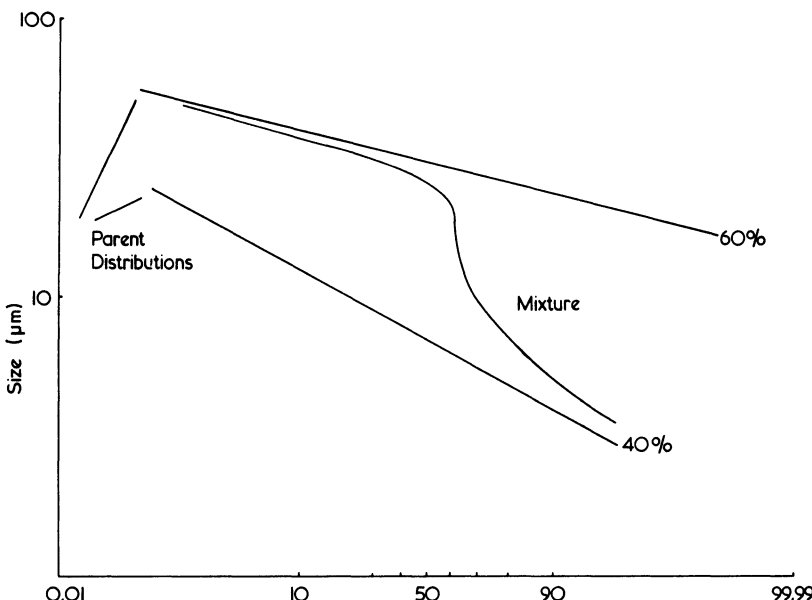


Figure 4.14 Bimodal non-intersecting distributions.

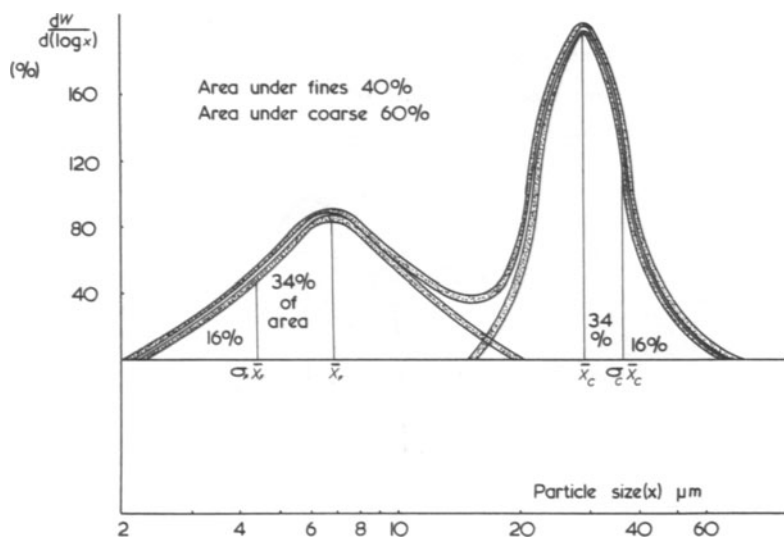


Figure 4.15 Relative percentage per log-micrometre of a bimodal distribution with little overlap.

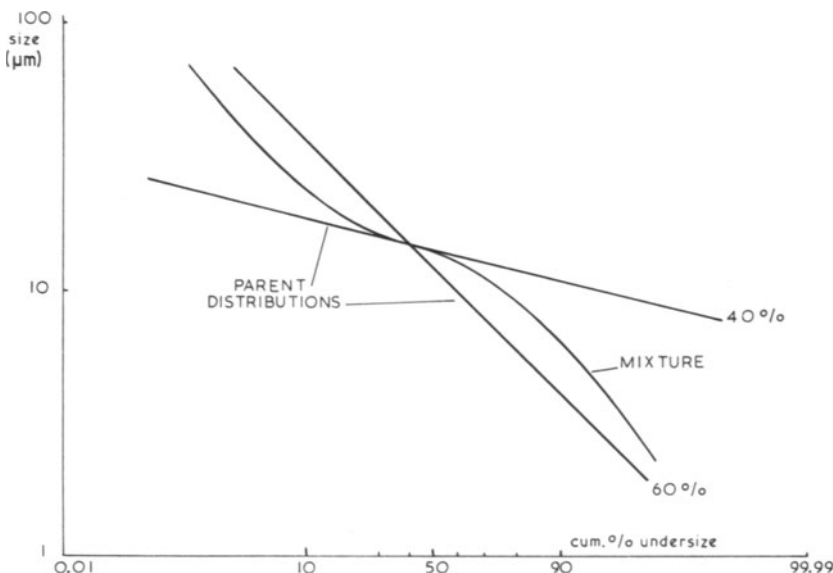


Figure 4.16 Bimodal intersecting distributions.

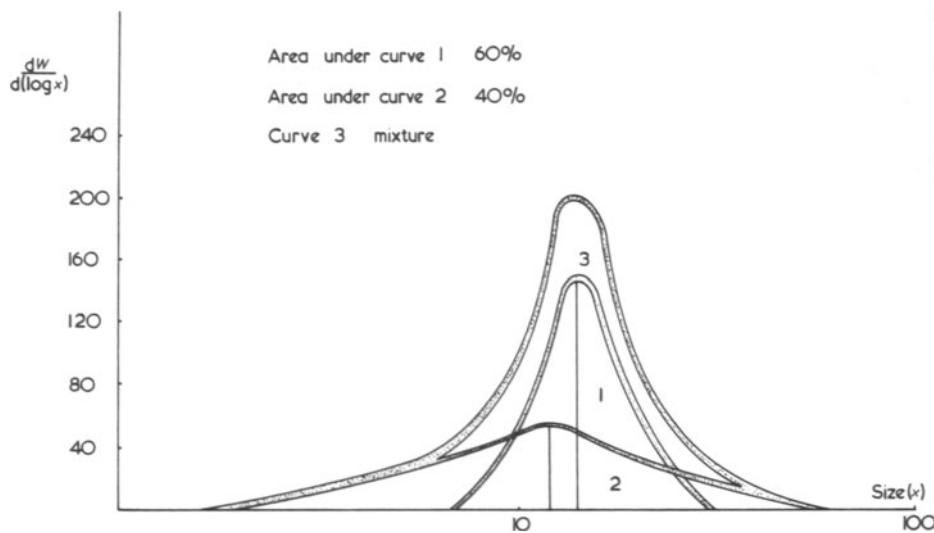


Figure 4.17 Relative percentage per log-micrometre of a bimodal distribution with small separation of means.

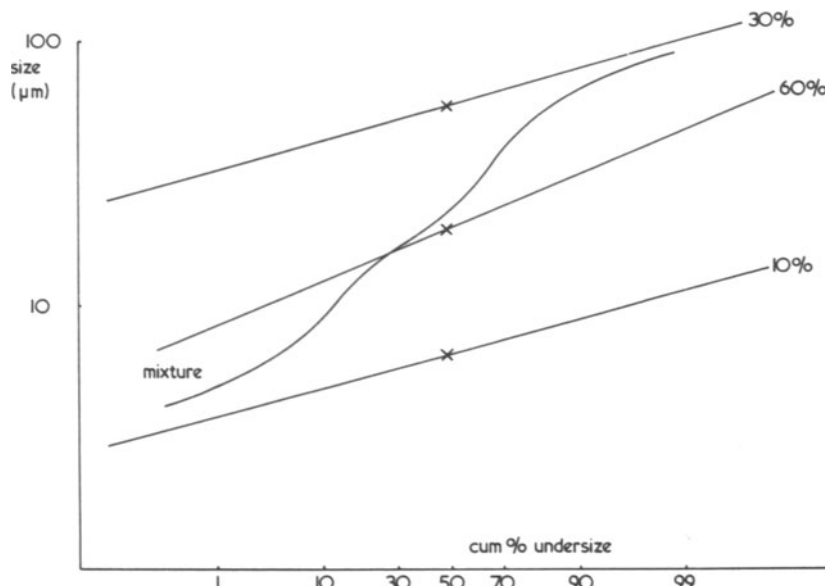


Figure 4.18 Trimodal distribution with parent distributions.

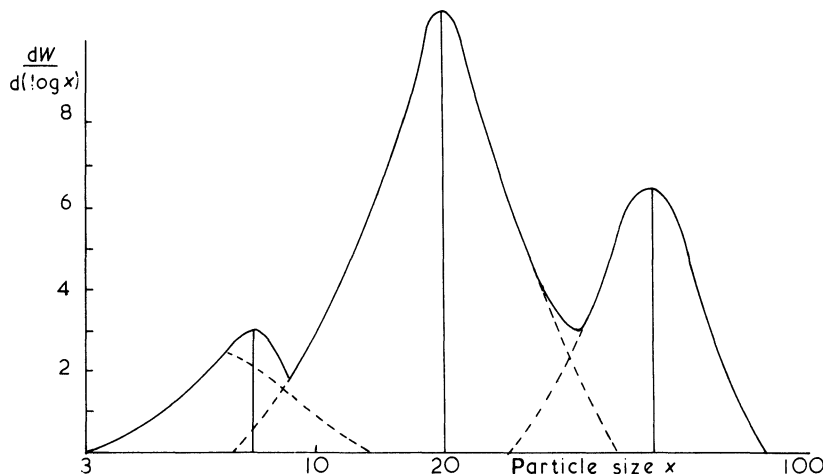


Figure 4.19 Relative percentage per log-micrometre of a trimodal distribution with little overlap.

4.8.8 Derivation of shape factors from parallel log-normal curves

The two curves on figure 4.20 are analyses of the same powder using gravimetric (X-ray and pipette sedimentation) and volumetric (Coulter) techniques.

Multiplying the diameter by the latter technique by a factor of 1.27 brings the two curves into coincidence, hence:

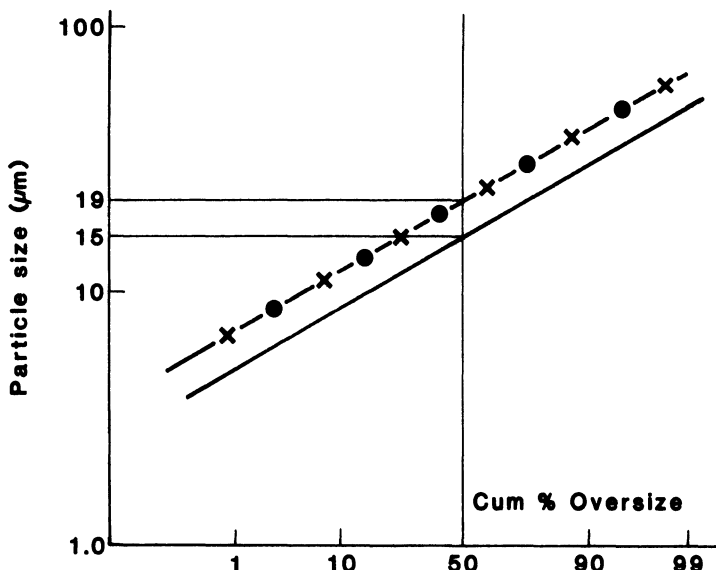


Figure 4.20 Comparison between Coulter and X-ray (x) and pipette methods (●).

$$1.27d_{St} = d_v$$

Since: $d_{St}^2 \div \frac{d_v^3}{d_s}$

this gives:

$$\frac{d_v}{d_{St}} = 1.27; \quad \frac{d_s}{d_v} \div 1.27^2$$

and, from equation (4.17):

$$\psi_w = 0.384$$

For a spherical particle, these ratios are unity, increasing with increasing divergence from sphericity.

4.9 THE LAW OF COMPENSATING ERRORS

In any method of size analysis, it is always possible to assign the wrong size to some of the particles. If this error is without bias, the possibility of assigning too great a size is equally as probable as assigning too small a size. This will modify the extremes of the distribution, but will have little effect on the central region. An illustration with particles of mean size 1, $\sqrt{2}$, 2, $2\sqrt{2}$, 4,

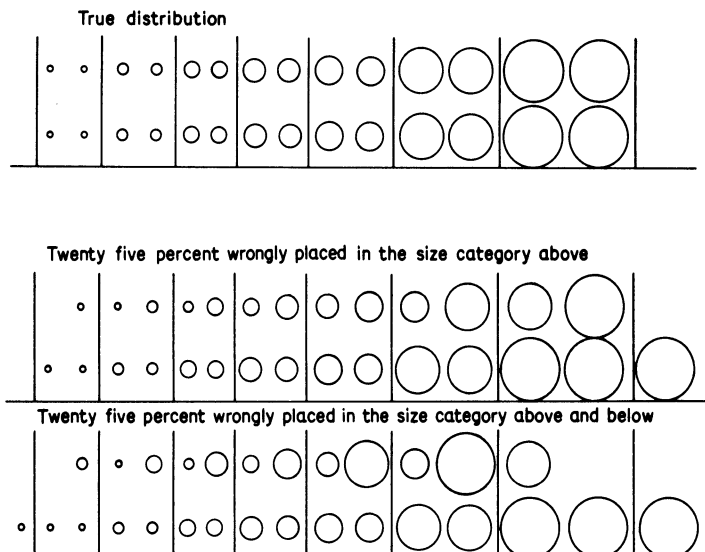


Figure 4.21 Law of compensating variables.

$4\sqrt{2}$, 8, in which 25% in each size range are placed in the size category below and 25% in the size category above, is shown in figure 4.21. An illustration with bias is also shown with particles having the same size ranges as in the first example, but with 25% in each category being placed in the category above.

It can be seen that there is the same number of particles in each of the central-size categories, irrespective of whether bias is present or not. If the number distribution is converted into a weight distribution, this is still true, but wrongly assigning a size of $8\sqrt{2}$ to 25% by number of the particles in the top-size category gives an apparently coarser distribution. For measurement sizes in arithmetic progression of sizes, the effect is small provided sizing is carried out at 10 or more size intervals and, for a log-normal distribution plotted as a relative frequency curve against the logarithm of particle size, the position of the mode is only slightly affected.

Table 4.16 is for a long-normal distribution having a mean size of $8.6 \mu\text{m}$ and a standard deviation of 0.320. Wrongly placing 25% of each category by weight in the size category above and 25% in the size category below, gives a mean size of $8.6 \mu\text{m}$ and a standard deviation of 0.284.

Table 4.16

Upper size limit (μm)	Mean size (μm)	Cumulative percentage undersize		Percentage in range	
		true	error	true	error
1	1.2	0	0.08	0.3	0.08
$\sqrt{2}$	1.7	0.3	0.50	1.1	0.42
2	2.4	1.4	2.15	4.1	1.65
$2\sqrt{2}$	3.4	5.5	6.85	9.5	4.70
4	4.8	15.0	17.38	19.0	10.53
$4\sqrt{2}$	6.8	34.0	35.25	24.0	17.87
8	9.6	58.0	57.00	20.0	21.75
$8\sqrt{2}$	13.4	78.0	76.28	13.0	19.25
16	19.0	91.0	89.385	6.4	13.10
$16\sqrt{2}$	28.9	97.4	96.30	2.0	6.95
32	38.0	99.4	99.03	0.5	2.73
$32\sqrt{2}$	53.8	99.9	99.80	0.1	0.77
64	76.0	100	99.98		0.18
			100		0.02

Figure 4.22 shows a log-normal distribution of geometric mean size $10 \mu\text{m}$ and geometric standard deviation 2. This distribution is deficient in sub- $6 \mu\text{m}$ particles and is asymptotic to this size. If $(x - 6)$ is taken as the particle size, a straight line results to give the original distribution. A similar sort of plot occurs when there is a deficiency of coarse particles and this may be similarly resolved.

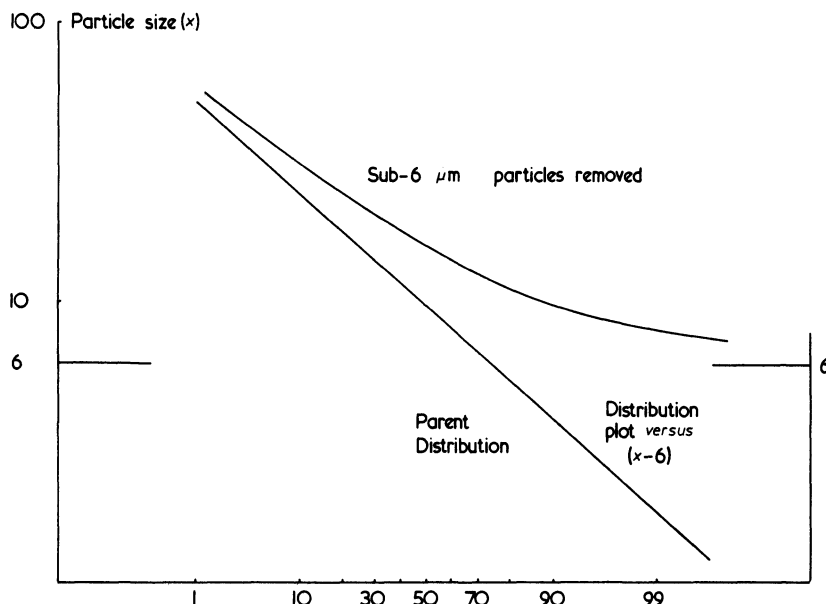


Figure 4.22 Log-normal distribution with deficiency of sub-6 μm particles.

Figure 4.23 shows Andreasen analysis monitoring a grinding operation. Since, in this case, the new surface created is proportional to grinding time, it is possible to predict future performance. Similarly, less accurately, maximum size is inversely proportional to grinding time (see table on p. 173).

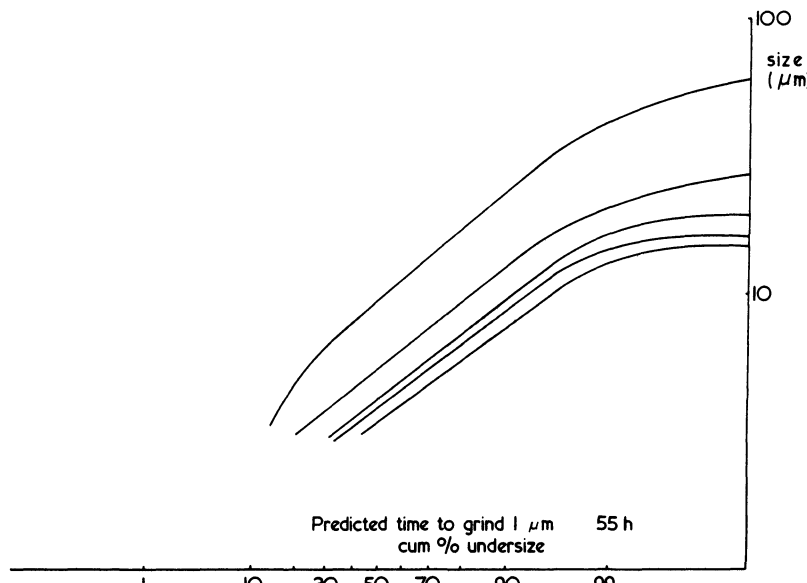


Figure 4.23 Andreasen analysis monitoring a grinding operation (1).

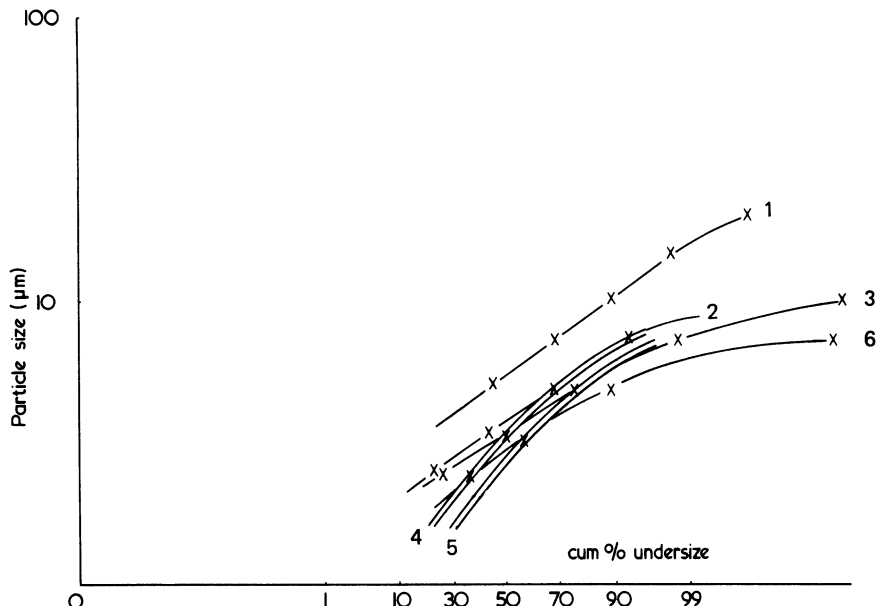


Figure 4.24 Andreasen analysis monitoring a grinding operation (2).

Grinding time t (hours)	Mean particle size (μm)	Maximum particle size x_g (μm)	$x_g t$	$x_m t$
9	5.3	27.5	47.7	239
13	4.1	19	53.3	247
15	3.75	16	56.3	240
16	3.42	14	54.7	224

Hence, the predicted time to grind to 1 μm mean size is 55 hours; the predicted time to produce sub-10 μm particles is 24 hours.

Figure 4.24 gives six analyses from a grinding operation. For samples 4 and 5, the grinding variables have been altered.

4.10 ALTERNATIVE NOTATION FOR FREQUENCY DISTRIBUTION

The notation used in this chapter is widely used but an alternative notation has been developed in Germany [41–47]. Although elegant, the German notation requires some memorization and is probably most suitable for fre-

quent usage and computer application. It is included here, in a shortened form, for the sake of completeness.

4.10.1 Notation

Let the fractional number smaller than size x be:

$$Q_0(x) = \int_{x_{\min}}^x q_0(x) dx \quad (4.68)$$

$$\text{or } q_0(x) = \frac{dQ_0(x)}{dx} \quad (4.69)$$

Hence $q_0(x)$ is the fractional number in the size range x to $x + dx$.

Further:

$$Q_0(x)_{\max} = \int_{x_{\min}}^{x_{\max}} q_0(x) dx = 1 \quad (4.70)$$

The subscript may be varied to accommodate other distributions, viz: q_r and Q_r where:

$r = 0$ for a number distribution

$r = 1$ for a length distribution

$r = 2$ for an area distribution

$r = 3$ for a volume distribution

4.10.2 Moment of a distribution

The moment of a distribution is written as:

$$M_{k,r} = \int_{x_{\min}}^{x_{\max}} x^k q_r(x) dx \quad (4.71)$$

[Note $M_{0,r} = 1$.]

For an incomplete distribution:

$$M_{k,r}(x_e, x_u) = \int_{x_e}^{x_u} x^k q_r(x) dx \quad (4.72)$$

4.10.3 Transformation from $q_t(x)$ to $q_r(x)$

If $q_t(x)$ is known $q_r(x)$ may be determined using the following:

$$\begin{aligned}
 q_r(x) &= \frac{x^{r-t} q_t(x)}{\int_{x_{\min}}^{x_{\max}} x^{r-t} q_t(x) dx} \\
 &= \frac{x^{r-t} q_t(x)}{M_{r-t,T}}
 \end{aligned} \tag{4.73}$$

The denominator is necessary to normalize the distribution function.

Examples

To convert from a number to a weight distribution put $t = 0$, $r = 3$. To convert from a surface to a weight distribution put $t = 2$, $r = 3$.

Effect of particle shape

This transformation is derived with the assumption that particle shape does not change with particle size. More correctly:

$$q_r(x) = \frac{\alpha(x) x^{r-t} q_t(x)}{\int_{x_{\min}}^{x_{\max}} \alpha(x) x^{r-t} q_t(x) dx} \tag{4.74}$$

where α is a shape coefficient.

4.10.4 Relation between moments

Putting $t = 0$ in equation (4.73) and substituting $q_0(x)$ for $q_r(x)$ in equation (4.71) gives:

$$\begin{aligned}
 M_{k,r} &= \frac{\int_{x_{\min}}^{x_{\max}} x^k x^r q_0(x) dx}{M_{r,0}} \\
 M_{k,r} &= \frac{M_{k+r,0}}{M_{r,0}}
 \end{aligned} \tag{4.75}$$

More generally, substituting $q_r(x)$ from equation (4.73) in equation (4.71) gives:

$$M_{k,r} = \frac{M_{k+r-t,t}}{M_{r-t,t}} \tag{4.76}$$

Examples

To determine the surface-volume mean diameter from a number distribution put $t = 0$, $r = 2$, $k = 1$:

$$M_{1,2} = \frac{M_{3,0}}{M_{2,0}} = x_{sv}$$

To determine the surface-volume mean diameter from a surface distribution put $t = 2$, $r = 2$, $k = 1$:

$$M_{1,2} = \frac{M_{1,2}}{M_{0,2}}$$

4.10.5 Means of distributions

(a) Distribution means are given by the equation:

$$\begin{aligned}\bar{x}_{1,r} &= \frac{\int_{x_{\min}}^{x_{\max}} x q_r(x) dx}{\int_{x_{\min}}^{x_{\max}} q_r(x) dx} \\ \bar{x}_{1,r} &= \frac{M_{1,r}}{M_{0,r}} = \frac{M_{r+1,0}}{M_{r,0}} \\ &= M_{1,r}\end{aligned}\tag{4.77}$$

(b) Arithmetic means are given by the equation:

$$\begin{aligned}\bar{x}_{k,0} &= \left[\frac{\int_{x_{\min}}^{x_{\max}} x^k q_0(x) dx}{\int_{x_{\min}}^{x_{\max}} q_0(x) dx} \right]^{1/k} \\ \bar{x}_{k,0} &= k \vee (M_{k,0})\end{aligned}\tag{4.78}$$

(c) More generally:

$$\begin{aligned}(\bar{x}_{k,r})^k &= \frac{\int_{x_{\min}}^{x_{\max}} x^k q_r(x) dx}{\int_{x_{\min}}^{x_{\max}} q_r(x) dx} \\ (\bar{x}_{k,r})^k &= M_{k,r}\end{aligned}\tag{4.79}$$

4.10.6 Standard deviations

For a number distribution, the variance is defined by:

$$\begin{aligned}\sigma_0^2 &= \int_{x_{\min}}^{x_{\max}} (x - \bar{x}_{1,0}) q_0(x) dx \\ &= \int_{x_{\min}}^{x_{\max}} x^2 q_0(x) dx - \bar{x}_{1,0}^2 \int_{x_{\min}}^{x_{\max}} q_0(x) dx \\ \sigma_0^2 &= M_{2,0} - (M_{1,0})^2\end{aligned}\tag{4.80}$$

More generally:

$$\begin{aligned}\sigma_r^2 &= \int_{x_{\min}}^{x_{\max}} (x - \bar{x}_{1,r})^2 q_r(x) dx \\ \sigma_r^2 &= M_{2,r} - (M_{1,r})^2\end{aligned}\tag{4.81}$$

Alternatively:

$$\sigma_r^2 = M_{1,r} \left[\frac{M_{2,r}}{M_{1,r}} - M_{1,r} \right]$$

Putting $t = r + 1$ and $k = 1$ in equation (4.76) gives:

$$\sigma_r^2 = M_{1,r} [M_{1,r+1} - M_{1,r}] \tag{4.82}$$

From equation (4.79):

$$\sigma_r^2 = \bar{x}_{1,r} [\bar{x}_{1,r+1} - \bar{x}_{1,r}] \tag{4.83}$$

4.10.7 Coefficient of variation

$$C_r^2 = \frac{\sigma_r^2}{(\bar{x}_{1,r})^2} \tag{4.84}$$

$$= \frac{\bar{x}_{1,r+1}}{\bar{x}_{1,r}} - 1 \tag{4.85}$$

4.10.8 Applications

(a) Calculation of volume-specific surface

$$S_v = \frac{\text{surface area}}{\text{volume}}$$

$$= \frac{\int_{x_{\min}}^{x_{\max}} \alpha_s(x) x^2 q_0(x) dx}{\int_{x_{\min}}^{x_{\max}} \alpha_v(x) x^3 q_0(x) dx}$$

where $\alpha_s(x)$ and $\alpha_v(x)$ are the surface and volume shape coefficients. Assuming that these are independent of particle size and defining the ratio of α_s to α_v as α_{sv} , the surface-volume shape coefficient is:

$$S_v = \alpha_{sv} \frac{M_{2,0}}{M_{3,0}} = \frac{\alpha_{sv}}{M_{1,2}} = \alpha_{sv} M_{1,3} \quad (4.86)$$

Also, since $M_{1,2} = \bar{x}_{1,2}$

$$S_v = \frac{\alpha_{sv}}{\bar{x}_{1,2}} \quad (4.87)$$

(b) Calculation of the surface area of a size increment

$$\begin{aligned} S_v(x_e, x_u) &= \frac{\int_{x_e}^{x_u} \alpha_s x^2 q_0(x) dx}{\int_{x_e}^{x_u} \alpha_v x^3 q_0(x) dx} \\ &= \alpha_{sv} \frac{M_{2,0}(x_e, x_u)}{M_{3,0}(x_e, x_u)} \\ &= \alpha_{sv} \left[\frac{M_{2,0}(x_e, x_u)}{M_{3,0}} \right] \times \left[\frac{M_{3,0}}{M_{3,0}(x_e, x_u)} \right] \end{aligned}$$

Now:

$$\begin{aligned} Q_r(x_i) &= \int_{x_{\min}}^{x_i} q_r(x) dx = \frac{\int_{x_{\min}}^{x_i} x^r q_0(x) dx}{M_{r,0}} \\ &= \frac{M_{r,0}(x_{\min}, x_i)}{M_{r,0}} \end{aligned}$$

so:

$$Q_3(x_u) - Q_3(x_e) = \frac{M_{3,0}(x_e, x_u)}{M_{3,0}}$$

hence:

$$S_v = \alpha_{sv} \left[\frac{M_{2,0}(x_e, x_u)}{M_{3,0}} \right] \times \left[\frac{1}{Q_3(x_u) - Q_3(x_e)} \right] \quad (4.88)$$

The application of this equation enables a surface area to be calculated from a summation of increments, i.e.

$$\begin{aligned} S_v &= \alpha_{sv} \frac{M_{2,0}}{M_{3,0}} \\ &= \frac{\alpha_{sv}}{M_{3,0}} \left[\int_{x_{\min}}^{x_{u_1}} x^2 q_0(x) dx + \int_{x_{u_1}}^{x_{u_2}} x^2 q_0(x) dx + \dots \right] \\ &= \frac{\alpha_{sv}}{M_{3,0}} \sum_{i=1}^{i=n} M_{2,0}(x_{e_i}, x_{u_i}) \end{aligned} \quad (4.89)$$

$e_i = \min$, $u_n = \max$.

4.10.9 Transformation of abscissa

Suppose, in an analysis, ξ , which is a function of x , is measured. Since the amount of material between sizes x and $x + dx$ is constant, there must be a simple relationship between $q(\xi)$ and $q(x)$. Let

$$x = f(\xi) \quad \text{so that} \quad \xi = \phi(x)$$

then

$$q_r^*(\xi) = q_r(x) \cdot \frac{dx}{d\xi} \quad (4.90)$$

For example, suppose the following relationship holds:

$$\xi = x^k$$

then

$$\frac{d\xi}{dx} = kx^{k-1}$$

and

$$q_r^*(\xi) = \frac{1}{kx^{k-1}} q_r(x) \quad (4.91)$$

In general, suppose we have the $q_u(x)$ distribution and wish to find the $q_r(x^k)$ distribution. Now from equation (4.73):

$$q_r(x) = \frac{x^{r-u} q_u(x)}{M_{r-u,u}}$$

Substituting in equation (4.91) gives:

$$q_r^*(\xi) = \frac{x^{r-u} q_u(x)}{M_{r-u,u}} \frac{1}{kx^{k-1}} \quad (4.92)$$

Example

In a Coulter counter analysis, the pulse height V is proportional to particle volume, i.e.

$$\xi = V = p^3 x^3$$

Calculation of $M_{r,0}$ ($= [\bar{x}_{r,0}]'$)

By definition:

$$\begin{aligned} M_{r,0} &= \int_{x_{\min}}^{x_{\max}} x^r q_0(x) dx \\ &= \frac{1}{p^r} \int_{q_{\min}}^{q_{\max}} \xi^{r/3} q_0^*(\xi) d\xi \\ &= \frac{M_{r/3,0}(\xi)}{p^r} \end{aligned} \quad (4.93)$$

Also, since $q_r(x) = \frac{x^r q_0(x)}{M_{r,0}}$

substituting in equations (4.90) and (4.94):

$$\begin{aligned} q_r(x) &= x^r q_r^*(\xi) \frac{d\xi}{dx} \cdot \frac{p^r}{M_{r/3,0}(\xi)} \\ q_r(x) &= \frac{3pq^{(r+2)/3} q_0^*(\xi)}{M_{r/3,0}(\xi)} \end{aligned} \quad (4.94)$$

To calculate $M_{k,r}$

$$\begin{aligned}
 M_{k,r} &= \int_{x_{\min}}^{x_{\max}} x^k q_r(x) dx \\
 &= \frac{1}{p^k} \int_{x_{\min}}^{x_{\max}} \frac{\xi^{(k+r)/3} q_0^*(\xi) d\xi}{M_{r/3,0}(\xi)} \\
 &= \frac{M_{(k+r)/3,0}(q)}{M_{r/3,0}(q)}
 \end{aligned} \tag{4.95}$$

To calculate volume-specific surface:

$$S_v = a_{sv} \frac{M_{2,0}}{M_{3,0}}$$

which, using equation (4.95), may be written:

$$S_v = a_{sv} \cdot p \frac{M_{2/3,0}(\xi)}{M_{1,0}(\xi)} \tag{4.96}$$

Thus, specific surface can be determined from moments calculated directly from Coulter counter data.

Calculation of mean size $\bar{x}_{k,r}$

$$\begin{aligned}
 \bar{x}_{k,r} &= k \vee(M_{k,r}) \\
 &= \frac{1}{p} k \sqrt{\left(\frac{M_{(k+r)/3,0}(\xi)}{M_{r/3,0}(\xi)} \right)}
 \end{aligned} \tag{4.97}$$

4.11 PHI-NOTATION

In geological literature dealing with particle size distribution, a very advantageous transformation of particle size is commonly used. Because it is a logarithmic transformation, it simplifies granulometric computations in the same way as logarithms in mathematical operations. This transformation replaces ratio scale numbers, based on millimetre values of particle size, by interval scale numbers, based on the logarithms of those values. Although several transformations based on decadic logarithms were also suggested (zeta-transformation [55] and gamma-transformation [48]) more than thirty years ago, it has been broadly adopted, particularly in the USA. After the redefinition by McManus [49] and the comments of Krumbein [11], the transformation is:

$$\phi = -\log_2 X_i \quad \text{or} \quad X_i = 2^{-\phi} \quad (4.98)$$

where X_i is a dimensionless ratio of a given particle size, in millimetres, to the standard particle size of 1 mm.

Phi-values can be found if the common decadic logarithms of X_i are multiplied by $(\log 10^2)^{-1} = 3.3219282$. Conversely, phi-values can be converted into their millimetre (or more precisely X_i) equivalents if their decadic anti-logarithms are multiplied by $\log 10^2 = 0.30103$. For easy manipulation, a conversion chart [50, p. 244] or a conversion table [51, 52] can be used.

By using the phi-notation, the statistical measurements acquire a great simplicity. The standard deviation, σ_ϕ , used in this notation refers to its quartile estimate:

$$\sigma_\phi = 0.5(\phi_{84} - \phi_{16}) \quad (4.99)$$

Similarly the ϕ skewness:

$$\phi = \frac{\phi_{16} + \phi_{84} - 2\phi_{50}}{\phi_{84} - \phi_{16}} \quad (4.100)$$

Other statistical measurements used in geology for particle size distribution characterization (moment, quartile and others) have been reviewed [53, 54].

4.12 MANIPULATION OF THE LOG-PROBABILITY EQUATION

Consider the log-normal equation:

$$\frac{d\phi}{d \ln x} = \frac{1}{\ln \sigma_g \sqrt{(2\pi)}} \exp \left[-\left(\frac{\ln x - \ln x_g}{\sqrt{2 \ln \sigma_g}} \right)^2 \right] \quad (4.101)$$

ϕ being a general term for the frequency, being number, length, surface or volume (weight) (i.e. $\phi = N, L, S$ or V).

$$\text{Let } X = \frac{(\ln x - \ln x_g)}{\sqrt{2 \ln \sigma_g}} \quad (4.102)$$

$$\text{then } \sqrt{2 \ln \sigma_g} \cdot dX = d \ln x \quad (4.103)$$

$$\text{and } \int d\phi = \frac{1}{\sqrt{\pi}} \int \exp(-X^2) dX \quad (4.104)$$

The fraction undersize the geometric mean size x_g is obtained by inserting the limits $x = 0, x = x_g$, i.e. $X = -\infty, X = 0$.

$$\begin{aligned}\phi_{x_g} &= \frac{1}{\sqrt{\pi}} \int_{-\infty}^0 \exp(-X^2) dX \\ &= \frac{1}{2}\end{aligned}\tag{4.105}$$

Therefore the geometric mean size is the median size.

The fraction lying within one standard deviation of the mean is obtained by inserting the limits $x = x_g$, $x = \sigma_g x_g$, i.e. $X = 0$, $X = 1/\sqrt{2}$.

$$\begin{aligned}\phi_{(x_g - \sigma_g x_g)} &= \frac{1}{\sqrt{\pi}} \int_0^{1/\sqrt{2}} \exp(-X^2) dX \\ &= \frac{1}{\sqrt{\pi}} \left[X - \frac{X^3}{3} + \frac{X^5}{10} - \frac{X^7}{42} + \dots \right]^* \\ &= 0.3413\end{aligned}\tag{4.106}$$

Hence 34.13% of the distribution lies between the median size x_g and size $\sigma_g x_g$. (Compare this to the normal-probability curve which contains 34.13% of the distribution between the sizes \bar{x} and $\bar{x} + \sigma$.) The geometric standard deviation is therefore: the ratio of the 84.13% and 50% sizes and the ratio of the 50% and 15.87% sizes:

$$\begin{aligned}\log \sigma_g x_g - \log x_g &= \log x_{84.13} - \log x_{50} \\ \sigma_g &= x_{84.13}/x_{50}\end{aligned}\tag{4.107}$$

4.12.1 Average sizes

Consider a log-normal distribution by number, such that:

$$\begin{aligned}{}^* \exp(-X^2) &= \lim_{n \rightarrow \infty} \left[1 + \left(\frac{-X^2}{n} \right) \right]^n \\ &= 1 + n \left(\frac{-X^2}{n} \right) + \frac{n(n-1)}{2!} \left(\frac{-X^2}{n} \right)^2 + \dots + \frac{n!}{(n-r)!r!} \left(\frac{-X^2}{n} \right)^r + \dots \\ \int \exp(-X^2) dX &= X - \frac{X^3}{3} + \frac{1}{2!} \frac{X^5}{5} - \frac{1}{3!} \frac{X^7}{7} + \dots \\ &\quad + \dots + \frac{(-1)^{r-1}}{(r-1)!} \frac{X^{2r-1}}{2r-1} \dots\end{aligned}$$

$$\int_{-\infty}^{+\infty} d\phi = \sum_{r=0}^{r=\infty} dN_r = \frac{1}{\ln \sigma_g \sqrt{(2\pi)}} \int_{-\infty}^{+\infty} \exp \left[-\left(\frac{\ln x - \ln x_{gN}}{\sqrt{2 \ln \sigma_g}} \right)^2 \right] d \ln x = 1 \quad (4.108)$$

i.e. the distribution is normalized.

dN_r is the number of particles, in a narrow size range, of mean size x_r ; x_0 and x_∞ are the smallest and largest particles present in the distribution. x_{gN} is the geometric mean (median) of the number distribution and σ_g is the geometric standard deviation (which is the same for number, length, surface and weight).

$$x_{NL} = \frac{\sum_{r=0}^{r=\infty} x_r dN_r}{\sum_{r=0}^{r=\infty} dN_r} = \frac{\sum_{r=0}^{r=\infty} x_r dN_r}{\int_{-\infty}^{+\infty} \exp \left[-\left(\frac{\ln x - \ln x_{gN}}{\sqrt{2 \ln \sigma_g}} \right)^2 \right] x d \ln x} \quad (4.109)$$

$$x_{NS}^2 = \sum_{r=0}^{r=\infty} x_r^2 dN_r = \frac{1}{\ln \sigma_g \sqrt{(2\pi)}} \int_{-\infty}^{+\infty} \exp \left[-\left(\frac{\ln x - \ln x_{gN}}{\sqrt{2 \ln \sigma_g}} \right)^2 \right] x^2 d \ln x \quad (4.110)$$

$$x_{NV}^3 = \sum_{r=0}^{r=\infty} x_r^3 dN_r = \frac{1}{\ln \sigma_g \sqrt{(2\pi)}} \int_{-\infty}^{+\infty} \exp \left[-\left(\frac{\ln x - \ln x_{gN}}{\sqrt{2 \ln \sigma_g}} \right)^2 \right] x^3 d \ln x \quad (4.111)$$

Substituting from equations (4.102) and (4.103) gives:

$$x_{NL} = \frac{x_{gN}}{\sqrt{\pi}} \int_{-\infty}^{+\infty} \exp(\sqrt{2 \ln \sigma_g} X - X^2) dx \quad (4.112)$$

$$x_{NS}^2 = \frac{x_{gN}^2}{\sqrt{\pi}} \int_{-\infty}^{+\infty} \exp(2\sqrt{2 \ln \sigma_g} X - X^2) dx \quad (4.113)$$

$$x_{NV}^3 = \frac{x_{gN}^3}{\sqrt{\pi}} \int_{-\infty}^{+\infty} \exp(3\sqrt{2 \ln \sigma_g} X - X^2) dx \quad (4.114)$$

Making the transformations:

$$Y_1 = X - \frac{\sqrt{2}}{2} \ln \sigma_g \text{ in equation (4.112)}$$

$$Y_2 = X - \sqrt{2} \ln \sigma_g \text{ in equation (4.113)} \quad (4.115)$$

$$Y_3 = X - \frac{3\sqrt{2}}{2} \ln \sigma_g \text{ in equation (4.114)} \quad (4.116)$$

$$x_{NL} = \frac{x_{gN}}{\sqrt{\pi}} \exp\left(\frac{1}{2} \ln^2 \sigma_g\right) \int_{-\infty}^{+\infty} \exp(-Y_1^2) dY_1 \quad (4.117)$$

$$x_{NS}^2 = \frac{x_{gN}^2}{\sqrt{\pi}} \exp(2 \ln^2 \sigma_g) \int_{-\infty}^{+\infty} \exp(-Y_2^2) dY_2 \quad (4.118)$$

$$x_{NV}^3 = \frac{x_{gN}^3}{\sqrt{\pi}} \exp\left[\left(\frac{9}{2}\right) \ln^2 \sigma_g\right] \int_{-\infty}^{+\infty} \exp(-Y_3^2) dY_3 \quad (4.119)$$

The integration yields a value $I = \sqrt{\pi}$ giving:

$$\ln x_{NL} = \ln x_{gN} + 0.5 \ln^2 \sigma_g \quad (4.120)$$

$$2 \ln x_{NS} = 2 \ln x_{gN} + 2 \ln^2 \sigma_g \quad (4.121)$$

$$3 \ln x_{NV} = 3 \ln x_{gN} + 4.5 \ln^2 \sigma_g \quad (4.122)$$

Similarly:

$$4 \ln x_{NM} = 4 \ln x_{gN} + 8 \ln^2 \sigma_g \quad (4.123)$$

4.12.2 Derived average sizes

If the number-size distribution of a particulate system has been determined and found to be log-normal, equations (4.109) to (4.112) may be used to determine other average sizes.

For example, the mean size of a weight distribution is given by:

$$x_{VM} = \frac{\sum_{r=0}^{r=\infty} x_r^4 dN_r}{\sum_{r=0}^{r=\infty} x_r^3 dN_r} \\ = \frac{x_{NM}^4}{x_{NV}^3}$$

$$\text{Therefore } \ln x_{VM} = 4 \ln x_{NM} - 3 \ln x_{NV} \quad (4.124)$$

Substituting from equations (4.122) and (4.123):

$$\ln x_{VM} = \ln x_{gN} + 3.5 \ln^2 \sigma_g \quad (4.125)$$

Similarly, the mean size of a surface distribution is given by:

$$\ln x_{SV} = \ln x_{gN} + 2.5 \ln^2 \sigma_g \quad (4.126)$$

Using this equation, the specific surface of the particulate system may be determined since:

$$S_V = 6/x_{SV} \quad (4.127)$$

4.12.3 Transformation of the log-normal distribution by count into one by weight

If a number distribution is log-normal, the weight distribution is also log-normal with the same geometric standard deviation. Using the same treatment as was used to derive equation (4.109) gives, for a weight analysis:

$$\ln x_{VM} = \ln x_{gV} + \frac{1}{2} \ln^2 \sigma_g \quad (4.128)$$

Comparing with equation (4.114) gives:

$$\ln x_{gV} = \ln x_{gN} + 3.0 \ln^2 \sigma_g \quad (4.129)$$

Since the relations between the number-average sizes and the number-geometric mean are known (equations (4.120) to (4.123)), these can now be expressed as relationships between number-average sizes and the weight (volume) geometric mean x_{gV} .

$$\ln x_{NL} = \ln x_{gV} - 2.5 \ln^2 \sigma_g \quad (4.130)$$

$$\ln x_{NS} = \ln x_{gV} - 2.0 \ln^2 \sigma_g \quad (4.131)$$

$$\ln x_{NV} = \ln x_{gV} - 1.5 \ln^2 \sigma_g \quad (4.132)$$

$$\ln x_{NM} = \ln x_{gV} - 1.0 \ln^2 \sigma_g \quad (4.133)$$

Other average sizes may be derived from the above, using a similar procedure to that used to derive equations (4.125) and (4.126) to give:

$$\ln x_{SV} = \ln x_{gV} - 0.5 \ln^2 \sigma_g \quad (4.134)$$

Similarly, for a surface distribution, the equivalent equation to equation (4.129) is:

$$\ln x_{gS} = \ln x_{gN} + 2.0 \ln^2 \sigma_g \quad (4.135)$$

Substituting this relationship into equations (4.130) to (4.133) yields the equivalent relationships relating surface-average sizes with the surface-geometric mean diameter.

4.13 RELATIONSHIP BETWEEN MEDIAN AND MODE OF A LOG-NORMAL DISTRIBUTION

The log-normal equation may be written:

$$\frac{d\phi}{dx} = \frac{1}{x \ln \sigma_g \sqrt{2\pi}} \exp(-x^2)$$

where

$$2 \ln^2 \sigma_g X^2 = (\ln x - \ln x_g)^2$$

$$\sqrt{2 \ln \sigma_g} \frac{dX}{dx} = \frac{1}{x}$$

At the mode:

$$\frac{d^2\phi}{dx^2} = 0 = -\sqrt{2}X - \ln \sigma_g$$

$$\text{i.e. } \ln x_m = \ln x_g - \ln^2 \sigma_g \quad (4.136)$$

where x_m is the mode.

4.14 AN IMPROVED EQUATION AND GRAPH PAPER FOR LOG-NORMAL EVALUATIONS [56]

Using the relationship:

$$\frac{1}{x} = \exp(-\ln x) \quad (4.137)$$

equation (4.101) may be transformed into the following form:

$$\begin{aligned}\frac{d\phi}{dx} &= \frac{1}{\ln \sigma_g \sqrt{(2\pi)}} \exp(-\ln x) \exp\left[-\frac{1}{2 \ln^2 \sigma_g} \left(\ln \frac{x}{x_g}\right)^2\right] \\ &= \frac{1}{\ln \sigma_g \sqrt{(2\pi)}} \exp\left[-\frac{1}{2 \ln^2 \sigma_g} \{2 \ln^2 \sigma_g \ln x + (\ln x - \ln x_g)^2\}\right] \\ \{\} &= \ln^2 x - 2 \ln x (\ln^2 x_g - \ln^2 \sigma_g) + \ln^2 x_g\end{aligned}$$

Replacing x_g by x_m (equation (4.136)):

$$\{\} = 2 \ln x_m \ln^2 \sigma_g + \ln^4 \sigma_g + (\ln x - \ln x_m)^2$$

Therefore

$$\left[\right] = -\ln x_m - \frac{\ln^2 \sigma_g}{2} - \frac{(\ln x - \ln x_m)^2}{2 \ln^2 \sigma_g}$$

Hence:

$$\frac{d\phi}{dx} = \frac{1}{x_m \ln \sigma_g \sqrt{(2\pi)}} \exp\left(-\frac{1}{2} \ln^2 \sigma_g\right) \exp\left[-\frac{\ln^2 x/x_m}{2 \ln^2 \sigma_g}\right]$$

This form of the log-normal equation is more convenient for use since the variable only appears once. It may be simplified further:

$$\frac{d\phi}{dx} = A \exp(-b \ln^2 x/x_m) \quad (4.138)$$

$$\text{where } b = \frac{1}{2 \ln^2 \sigma_g}$$

$$\text{and } A = \sqrt{\frac{b}{\pi}} \cdot \frac{\exp(-1/4b)}{x_m}$$

The relationship between geometric mean and mode (equation (4.136)) takes the form:

$$C = \frac{x_m}{x_g} = \exp\left(-\frac{1}{2b}\right)$$

This modified form of the log-normal equation simplifies parameter determination from log-probability plots of experimental data. The graph paper may be furnished with additional scales of b and C both being determined by drawing a line parallel to the distribution through the pole (0.25 µm, 50%).

4.14.1 Applications

Consider a log-normal distribution with a geometric mean

$$x_g = 6.75 \mu\text{m}$$

and

$$\sigma_g = \frac{x_{84\%}}{x_{50\%}} = \frac{11.1}{6.75} = 1.64$$

The mode, according to equation (4.136), is:

$$x_m = 5.27 \mu\text{m}$$

making:

$$\frac{d\phi}{dx} = 0.1344 \exp \left[-2.02 \ln^2 \frac{x}{5.27} \right]$$

This form is particularly useful when further mathematical computation is envisaged such as for grade efficiency, $G_c(x)$, calculation since:

$$\begin{aligned} G_c(x) &= E_T \frac{dF_c(x)}{dF(x)} \\ &= E_T \frac{d\phi_c}{dx} \end{aligned}$$

where $d\phi_c/dx$ is the relative frequency of the coarse product, $d\phi/dx$ is the relative frequency of the feed and E_T is the total efficiency.

REFERENCES

- 1 Tsubaki, J. and Jimbo, G. (1979), *Powder Technol.*, **22**, 2, 161–70.
- 2 Heywood, H. (1947), Symposium on *Particle Size Analysis*, Inst. Chem. Engrs, Suppl. 25, 14.
- 3 Heywood, H. (1963), *J. Pharm. Pharmac.*, Suppl. 15, 56T.
- 4 Heywood, H. (1973), *Harold Heywood Memorial Lectures*, Loughborough University, England.
- 5 Wadell, H. (1932), *J. Geol.*, **40**, 243–53.
- 6 Wadell, H. (1935), *ibid.*, **43**, 250–80.
- 7 Wadell, H. (1934), *J. Franklin Inst.*, **217**, 459.
- 8 Wadell, H. (1934), *Physics*, **5**, 281–91.
- 9 Krumbein, W.C. (1934), *J. Sediment. Petrol.*, **4**, 65.
- 10 Krumbein, W.C. (1941), *ibid.*, **11**, 2, 64–72.

- 11 Krumbein, W.C. (1964), *ibid.*, **34**, 195.
- 12 Hausner, H.H. (1966), *Planseeber Pulvermetall.*, **14**, 2, 74–84.
- 13 Medalia, A.I. (1970/71), *Powder Technol.*, **4**, 117–38.
- 14 Church, T. (1968/69), *ibid.*, **2**, 27–31.
- 15 Cole, M. (June 1971), *Am. Lab.*, 19–28.
- 16 Pahl, M.H., Schädel, G. and Rumpf, H. (1973), *Aufbereit. Tech.*, **5**, 257–64; **10**, 672–83; **11**, 759–64.
- 17 Davies, R. (1975), *Powder Technol.*, **12**, 111–24.
- 18 Beddow, J.K. (1974), Report A390–CLME–74–007, The University of Iowa, 52242.
- 19 Laird, W.E. (1971), *Particle Technology*, Proc. Seminar, Indian Inst. Technol., Madras (eds D. Venkateswarlu and A. Prabhakdra Rao), 67–82.
- 20 Cartwright, J. (1962), *Ann. Occup. Hyg.*, **5**, 163.
- 21 Fair, G.L. and Hatch, L.P. (1933), *J. Am. Wat. Wks. Ass.*, **25**, 1551.
- 22 Crowl, V.T. (1963), Paint Research Station Report, No. 325, Teddington, London.
- 23 Ellison, J.McK. (1954), *Nature*, **173**, 948.
- 24 Hodkinson, J.R. (1962), PhD Thesis, London University.
- 25 Tsubaki, J. and Jimbo, G. (1979), *Powder Technol.*, 161–78.
- 26 Tsubaki, J., Jimbo, G. and Wade, R. (1975), *J. Soc. Mat. Sci. Japan*, **24**, 262, 622–6.
- 27 Schwarcz, H.P. and Shane, K.C. (1969), *Sedimentology*, **13**, 213–31.
- 28 Meloy, T.P. (1969), *Screening*, AIME, Washington, D.C.
- 29 Meloy, T.P. (1971), *Eng. Found. Conference*, Deerfield.
- 30 Meloy, T.P. (1977), *Powder Technol.*, **16**, 2, 233–54.
- 31 Meloy, T.P. (1977), *ibid.*, **17**, 1, 27–36.
- 32 Gotoh, K. and Finney, J.L. (1975), *ibid.*, **12**, 2, 125–30.
- 33 Mandelbrot, B.P. (1977), *Fractal Form Chance and Dimension*, W.H. Freeman & Co., San Francisco.
- 34 Kaye, B.H. (1977), *Proc. Particle Size Analysis Conference*, Salford, Chem. Soc., Analyt. Div., London.
- 35 Flook, A.G. (1978), *Powder Technol.*, **21**, 2, 295–8.
- 36 Medalia, A.J. (1970/71), *ibid.*, **4**, 117–38.
- 37 Morony, M.J., *Facts from Figures*, Pelican.
- 38 Herdan, G. (1960), *Small Particle Statistics*, Butterworths.
- 39 Irani, R.R. and Callis, C.F. (1963), *Particle Size: Interpretation and Applications*, Wiley, NY.
- 40 Rosin, P. and Rammler, E. (1933), *J. Inst. Fuel*, **7**, 29; (1927), *Zemast*, **16**, 820, 840, 871, 897; (1931), *Zemast*, **20**, 210, 240, 311, 343.
- 41 Rumpf, H. and Ebert, K.F. (1964), *Chem. Ingr. Tech.*, **36**, 523–37.
- 42 Rumpf, H. and Debbas, S. (1966), *Chem. Eng. Sci.*, **21**, 583–607.
- 43 Rumpf, H. and Debbas, S. and Schönert, K. (1967), *Chem. Ingr. Tech.*, **39**, 3, 116–25.
- 44 Rumpf, H. (1961), *ibid.*, **33**, 7, 502–8.
- 45 Leschonski, K., Alex, W. and Koglin, B. (1974), *ibid.*, **46**, 3, 23–6.
- 46 DIN 66141, February 1974.
- 47 Leschonski, K., Alex, W. and Koglin, B. (1974), *Chem. Ingr. Tech.*, **46**, 3, 101–6.
- 48 Baturin, V.P. (1943), *Reports Acad. Sci. USSR (Moscow)*, **38**, 7 (in Russian).
- 49 McManus, D.A. (1963), *J. Sediment. Petrol.*, **33**, 670.
- 50 Krumbein, W.C. and Pettijohn, F.J. (1938), *Manual of Sedimentary Petrography*, Appleton-Century-Crofts, New York.
- 51 Page, H.G. (1955), *J. Sediment. Petrol.*, **25**, 285.
- 52 Griffiths, J.C. and McIntyre, D.D. (1958), *A Table for the Conversion of Milli-*

- metres to Phi Units, Mineral Ind. Expl. Sta., Pennsylvania State University.
- 53 Folk, R.L. (1966), *Sedimentology*, **6**, 73.
- 54 Griffiths, J.C. (1962), In *Sedimentary Petrography* (ed. H.B. Milnes), 1, Macmillan, New York, Ch. 16.
- 55 Krumbein, W.C. (1937), *Neues Jahrb. Mineral Geol. Beil-Bd*, **73A**, 137–50.
- 56 Svarovsky, L. (1973), *Powder Technol.*, **7**, 6, 351–2.
- 57 Cartwright, J. (1962), *Ann. Occup. Hyg.*, **5**, 163–71.
- 58 Johnston, J.E. and Rosen, L.J. (1976), *Powder Technol.*, **14**, 195–201.
- 59 Schurt, G.A. and Johnston, J.E. (1975), *Proc. 13th AEC Air Cleaning Conference*, CONF-740807, 2, UC-70, 1039–44.
- 60 Gates, A.O. (1915), *Trans. AIME*, **52**, 875–909.
- 61 Schumann, R. (1940), *ibid.*, Tech. publ. 1189.
- 62 Gaudin, A.M. and Meloy, T.P. (1962), *ibid.*, 43–50.
- 63 Austin, L.R. and Klimpel, R.R. (1968), *Trans. Soc. Mech. Engrs*, 219–24.
- 64 Harris, C.C. (1969), *Trans. AIME*, **244**, 187–90.
- 65 Svensson, J. (1955), *Acta Polytech. Scand.*, **167**, 53.
- 66 Tarjan, G. (1974), *Powder Technol.*, **10**, 73–6.
- 67 Kolmogoroff, A.N. (1941), *Dokl. Akad. Nauk SSSR, Novaja Ser.*, **31**, 2.
- 68 Stein, F. and Corn, M. (1976), *Powder Technol.*, **13**, 133–41.
- 69 Narva, O.M. et al. (1977), *Zavod. Lab.*, **43**, 4, 477–8.
- 70 Naylor, A.G. and Kaye, B.H. (1972), *J. Colloid. Interfac. Sci.*, **39**, 1, 103–8.
- 71 White, E.T. et al. (1972), *Powder Technol.*, **5**, 2, 127–30.
- 72 Kaye, B.H. and Treasure, C.R.G. (1966), *Br. Chem. Engng*, **11**, 1220.
- 73 Seidel, H. (1966), *Staub*, **26**, 329.
- 74 Wise, M.E. (1954), *Philips Res. Rep.*, **9**, 231.
- 75 Petersen, E.E., Walker, P.L. and Wright, C.C. (1952), *ASTM Bull. TP 116*.
- 76 *Reporting Particle Size Characteristics of Pigments* (1955), *ASTM D1366-55T*.
- 77 Scott, K.J. and Mumford, D. (1971), *CSIR Spec. Rep. Chem.* 155, Pretoria, South Africa.
- 78 Martin, P.M. and Mills, A.A. (1977), *Moon* (Netherlands), **16**, 2, 215–19.
- 79 Beddow, J.K., Sisson, K. and Vetter, Q.F. (1976), *Powder Metall. Int.*, **2**, 69–76; **3**, 107–9.
- 80 Tracey, V.A. and Llewelyn, D.M. (1976), *ibid.*, **8**, 3, 126–8.
- 81 Beddow, J.K., *Powtech 77*, Heyden.
- 82 Beddow, J.K., Philip, G.C. and Nasta, M.D. (1975), *Planseeber. Pulvermetall.*, **23**, 3–14.
- 83 Beddow, J.K. et al. (1976), 8th Ann. Mtg. Fine Particle Soc., Chicago.
- 84 Mandelbrot, B.B. (1977), *Fractals: Form, Chance and Dimension*, W.H. Freeman, San Francisco, California, USA; Reading, UK.